(1)

PHILCO

PHILCO-FORD CORPORATION
Aeronutronic Division
Newport Beach, California

14

Publication No. U-3203

SCIENTIFIC REPORT

THE SHAPES OF COLLISION-BROADENED CO_2 LINES

Prepared for: Advanced Research Projects Agency
Washington, D.C.

Under Contract: NOnr 3560(00)
ARPA Order No. 237
Amendment No. 26/9-1-67

Prepared by: Darrell E. Burch
David A. Gryvnak
Richard R. Patty
Charlotte E. Bartky

Approved:

Paul M. Sutton

Paul M. Sutton, Manager
Physics and Chemistry Laboratories

31 August 1968

PHILCO
PHILCO-FORD CORPORATION
Aeronutronic Division
Newport Beach, Calif. • 92663

ABSTRACT

The shapes of the extreme wings of self-broadened CO_2 lines have been investigated in three spectral regions near 7000, 3800, and 2400 cm^{-1}. Absorption measurements have been made on the high-wavenumber sides of band heads where much of the absorption by samples at a few atm is due to the extreme wings of strong lines whose centers occur below the band heads. Considerable new information has been obtained about the shapes of self-broadened CO_2 lines as well as CO_2 lines broadened by N_2, O_2, A, He, and H_2. Beyond a few cm^{-1} from the line centers, all the lines absorb considerably less than Lorentz-shaped lines having the same half-widths. The deviation from the Lorentz shape decreases with increasing wavenumber in going from one of the three spectral regions to the next. The absorption by the wings of H_2- and He-broadened lines is particularly low, and the absorption decreases with increasing temperature at a faster rate than predicted by existing theories.

TABLE OF CONTENTS

ILLUSTRATIONS

ILLUSTRATIONS (Continued)

INTRODUCTION AND BACKGROUND

The shapes of spectral absorption lines has been the subject of considerable study since Michelson[1] wrote a paper dealing with the broadening of spectral lines in 1895. The two major factors leading to the broadening of spectral lines of gases are Doppler broadening and collision broadening, which is also frequently referred to as pressure broadening. Doppler broadening arises from the motion of the individual molecules in a gas and is dominant for gases at high temperatures or at very low pressures. Collision broadening is related to the pressure, or to the number of collisions, and is dominant for infrared absorption lines when the gas is at room temperature and at pressures greater than a few hundredths of an atm. The mechanism involved in Doppler broadening is relatively simple so that it is possible to calculate accurately the true shape of a Doppler-broadened line. However, this is not the case for collision-broadened lines since present theories do not adequately explain many of the features which have been observed.

Lack of good experimental data on the shapes of spectral lines is probably the major cause for the shortcomings of the theory at this point. It is experimentally difficult to observe the true shape of infrared lines because of the finite spectral slitwidth of spectrometers used to make the measurements. At low pressure, the transmittance near the center of a typical line changes so rapidly with wavenumber that the true contour cannot be observed. At high pressures, the lines are usually so wide that overlapping by neighboring lines is important, and the contribution by an individual line cannot be determined. Although the true shape very close to the line center cannot be measured directly with spectrometers, considerable information about the shapes of the lines can be obtained by measuring their equivalent widths for samples covering large ranges of pressure and absorber thickness. The equivalent width of a line is equal to $\int A(\nu)d\nu$, where $A(\nu)$ is the observed absorptance. The results of measurements of this sort for several different gases indicate that the shape of a collision-broadened line near its center is at least similar to the well-known Lorentz line shape (Eq. (6)).

Benedict, Herman, Moore, and Silverman[2,3] have found that the wings of HCl and CO lines deviate significantly from the Lorentz line shape a few cm^{-1} from their centers. These gases were studied because the relatively wide spacing of their absorption lines make it possible to observe the contribution of a single line at a point a few cm^{-1} from its center. However, absorption by the extreme wings of lines of other gases of astrophysical interest is difficult to measure since the absorption at

any wavenumber is usually complicated by nearby lines. Exceptions to this occur near some of the CO_2 bands which arise from changes in the vibrational quantum number v_3 and have band heads in the R-branches. On the high-wavenumber side of such a band head the absorption is due to the extreme wings of the lines whose centers occur below the band head. Winters, Silverman, and Benedict (WSB)[4] have made use of this feature of the ν_3 band of CO_2 to investigate the shapes of the extreme wings of the lines. These workers have found that the wings of the CO_2 lines are quite sub-Lorentzian, i.e., they absorb considerably less than lines having the same half-width and the Lorentz shape. They have also found that the shapes of the wings of lines broadened by argon or N_2 are quite different from self-broadened lines.

The present investigation extends the WSB work to two other spectral regions near 3800 cm^{-1} and near 7000 cm^{-1}; it also includes an investigation of broadening by other foreign gases and some data on the influence of temperature on line shape. We have found the extreme wings of the lines to be sub-Lorentzian in all three spectral regions for several different broadening gases. The shapes of the lines also depend on the wavenumber and on temperature in a manner not explained by any theory known to the authors. Some very interesting results have also been obtained for broadening by two light gases, He and H_2.

EXPERIMENTAL AND ANALYTICAL METHODS

Spectral curves were obtained by using two different spectrometers in the three spectral regions. A Perkin-Elmer spectrometer, Model 112, with a LiF prism and thermocouple detector, was employed near 2400 cm^{-1}. The two spectral regions near 3800 cm^{-1} and 7000 cm^{-1} were investigated with a small grating spectrometer employing a PbS detector cooled with liquid nitrogen.

The samples used in the 2400 cm^{-1} region varied in pressure up to 1 atm and were contained in a multiple-pass absorption cell with a base length of approximately 29 meters. This cell as well as a shorter one with a 1-meter base length contained samples investigated in the other two spectral regions. The shorter one was used at pressures as high as 15 atm and at temperatures up to approximately 431°K. The 2400 cm^{-1} data were obtained before the shorter absorption cell was constructed;

therefore, the data in this spectral region do not contain any samples at high pressures or elevated temperatures. The apparatus and experimental techniques have been discussed in detail previously.[5]

Samples consisted of either pure CO_2 or mixtures of CO_2 with one of the following broadening gases: N_2, O_2, A, He, and H_2. The partial pressure of CO_2 is denoted by p and the total pressure by P. Partial pressures of the other gases are denoted by p_{N_2}, p_{O_2}, . . ., etc. All pressures are given in atm with standard pressure of 1 atm denoted by a superscript, such as p^o.

The geometrical path length of the radiation through the sample is given by L, and the absorber thickness u is given by

$$u(\text{atm cm}_{STP}) = p(\text{atm})\,[1+0.005p]\,L(\text{cm})\,273/\theta(^\circ\text{K}). \qquad (1)$$

The factor [1+0.005p] accounts for the non-linearity in the relation between the pressure and density of CO_2, and (273/θ) reduces the absorber thickness to standard temperature, 273°K.

T(ν) represents observed transmittance of a sample at wavenumber ν, and T'(ν) is the true transmittance that would be observed with infinite resolving power. The absorption coefficient K(ν) is related to T'(ν) by

$$T'(\nu) = \exp[-uK(\nu)], \quad \text{or} \quad K(\nu) = -\frac{1}{u}\ln T'(\nu). \qquad (2)$$

In a region of overlapping lines, K(ν) is the sum ($\sum_i k_i(\nu)$) of the absorption coefficients due to the individual lines.

The strength, S, of an individual line is related to $k(\nu)$ and a shape factor $f(\alpha, \nu-\nu_o)$ by

$$k(\nu) = S\, f(\alpha, \nu-\nu_o), \text{ where} \tag{3}$$

$$\int_{-\infty}^{\infty} f(\alpha, \nu-\nu_o) = 1, \text{ and} \tag{4}$$

$$S = \int_{-\infty}^{\infty} k(\nu)d\nu. \tag{5}$$

For a Lorentz line, which is generally agreed to be approximately correct for collision-broadened lines when $\nu-\nu_o$ is small,

$$f_L(\alpha, \nu-\nu_o) = \frac{1}{\pi} \frac{\alpha}{(\nu-\nu_o)^2 + \alpha^2}. \qquad \text{(Lorentz)} \tag{6}$$

When $(\nu-\nu_o) \gg \alpha$, Eq. (6) reduces to

$$f_L(\alpha, \nu-\nu_o) = \frac{\alpha}{\pi(\nu-\nu_o)^2}. \qquad \text{(for } (\nu-\nu_o) \gg \alpha) \tag{7}$$

We have found that when $(\nu-\nu_o) \gg \alpha$, the Lorentz shape is not appropriate; however, the shapes can be expressed by the following equation:

$$f(\alpha, \nu-\nu_o) \quad f_L(\alpha, \nu-\nu_o)\chi(\nu-\nu_o) \quad \frac{\chi(\nu-\nu_o)}{\pi} \frac{\alpha}{(\nu-\nu_o)^2 + \alpha^2}. \tag{8}$$

The correction factor $\chi(\nu-\nu_o)$ is probably very near unity within a few tenths of a cm^{-1} of the line center where the Lorentz shape is generally agreed to be valid. The next-to-last section of this paper deals with the shapes of lines broadened by several atm of gas at points where $(\nu-\nu_o)$ may be a few cm^{-1} yet not large in comparison to α. Under this condition, Eq. (8) is not appropriate unless χ is expressed as a function of α as well as $(\nu-\nu_o)$. However, χ can be expressed satisfactorily as a function of $(\nu-\nu_o)$ when $(\nu-\nu_o) \gg \alpha$, which is the case for most of the results presented in this paper. The primary objective of the present investigation has been to determine the functional relationship between $\chi(\nu-\nu_o)$ and $(\nu-\nu_o)$ for large $(\nu-\nu_o)$.

It is understood that k, K, T', T, f, and χ are functions of ν, $(\nu-\nu_o)$, or α as indicated previously. However, in order to simplify the equations and figures, we have omitted the appropriate indication of the variables upon which these functions depend.

Representative spectral curves in the 7000 cm^{-1} region are shown in Fig. 1. The location of the very sharp band head near 6988.6 cm^{-1} is apparent in Curve A, which represents a sample of relatively large absorber thickness and low pressure. Many of the stronger lines in the R-branch of this band are crowded together within a narrow interval a few cm^{-1} below the band head. No lines of any significance occur between the band head and 7100 cm^{-1}; therefore, the absorption indicated by Curves B and C in this region is due to the extreme wings of lines occurring below the band head.

At a distance a few times greater than α above the band head, the contribution to the absorption coefficient by a single line for a sample of pure CO_2 is given by

$$k_s = \frac{S\alpha\chi}{\pi(\nu-\nu_o)^2} = \frac{S\alpha_s^o p(1+0.005p)\chi}{\pi p^o(\nu-\nu_o)^2}, \tag{9}$$

where the subscript s denotes self broadening, and α_s^o is the half-width at 1 atm. Since α is proportional to the number density of the molecules, rather than to pressure, the factor (1+0.005p) is included to account for the non-linearity in the relationship between these two quantities. The total absorption coefficient is given by the sum of the contributions of all of the individual lines,

$$K_s = \sum_i k_{s,i} = \sum_i \frac{S_i \chi_{s,i}\, p(1+0.005p)\alpha_{s,i}^o}{\pi p^o(\nu-\nu_{o,i})^2}. \tag{10}$$

For a mixture of p atm of CO_2 and p_b atm of broadening gas, the total absorption coefficient is given by

$$K = -\frac{1}{u}\ln T'(\nu) = \frac{K_s^o p(1+0.005p)}{p^o} + \frac{K_b^o p_b}{p^o}$$

$$\sum_i \frac{S_i}{\pi} \frac{\alpha_{s,i}^o}{p^o(\nu-\nu_{o,i})^2} \left[\chi_{s,i} p(1+0.005p) + \left(\frac{\alpha_b^o}{\alpha_s^o}\right) \chi_{b,i} p_b \right]. \tag{11}$$

The subscript b denotes broadening by a non-absorbing broadening gas; a specific broadening gas such O_2 or N_2 will be denoted by the appropriate subscript. The normalized absorption coefficients K_s^o and K_b^o correspond to 1 atm pressure. The half-width of a CO_2 line broadened by 1 atm of a foreign gas b in a mixture with CO_2 when $p \ll p_b$ is denoted by α_b^o. The ratio of the normalized half-widths (α_b^o/α_s^o) is assumed to be the same for all lines for a given broadening gas. The non-linearity in the relationship between number density and pressure for the foreign broadening gases was negligible.

Since there are no absorption lines between the band head and 7100 cm^{-1}, the absorption coefficient K does not change rapidly, except very near the band head. Therefore, the true transmittance $T'(\nu)$ in this region closely approximates the transmittance $T(\nu)$ observed with our spectrometer. Values of K_s^o at several different wavenumbers were determined from spectral curves of pure CO_2 samples by substituting $T(\nu)$ for $T'(\nu)$ in Eq. (11) with $p_b = 0$. These values of K_s^o were then used in Eq. (11) with values of T from spectral curves for mixtures of CO_2 and a broadening gas in order to determine K_b^o.

Values of the line strengths, S, were calculated by use of the appropriate theoretical expressions[6,7] from experimentally determined strengths, S_ν, of the vibration-rotation bands. Values of α for all of the lines were determined from information discussed below. The absorption coefficient K for a particular wavenumber was calculated by substituting into Eq. (11) the appropriate values of α and S_i, along with assumed

values of χ. For a particular broadening gas, we assumed that χ was a slowly-changing function of $(\nu-\nu_{o,i})$ only, and that this function was the same for every line in any one of the three spectral regions. However, we found that each broadening gas required a different χ function in each of the three spectral regions. Each χ function was represented by a table of χ vs $(\nu-\nu_o)$ which served as input for a computer that was used to perform the calculations. Each table was modified on a trial-and-error basis until all the calculated values of K^o in a given spectral region agreed, within experimental error, with the observed values. We then assumed that the function represented by the table which gave satisfactory agreement was appropriate. More detailed information about the methods used to determine the line parameters is given in the following sections, along with a discussion of the influence that errors in the line parameters have on the derived values of χ.

SPECTRAL CURVES AND LINE PARAMETERS

Representative spectral curves of the three regions investigated are shown in Figs. 1, 2, and 3. The shapes of the extreme wings of the lines occurring below the band head at 6988.6 cm^{-1} were investigated by measuring the absorption above the band head by samples such as those represented in Fig. 1. No absorption lines of any significance occur in the region between the band head and 7100 cm^{-1}. Essentially all the absorption in this region is due to the extreme wings of the lines of the $00^{0}3$ band and the weaker $01^{1}3$-$01^{1}0$ band whose head can be seen near 6950 cm^{-1}.

Curve B in Fig. 1 represents a 2 atm sample with sufficiently large u to produce significant absorption above the band head. Curve C, which represents a sample at 14.6 atm, is relatively smooth below 6900 cm^{-1} since the individual lines have been broadened sufficiently at the higher pressure to smooth-out the structure. It is of interest that Sample B absorbs more than Sample C below 6900 cm^{-1} since the absorber thickness

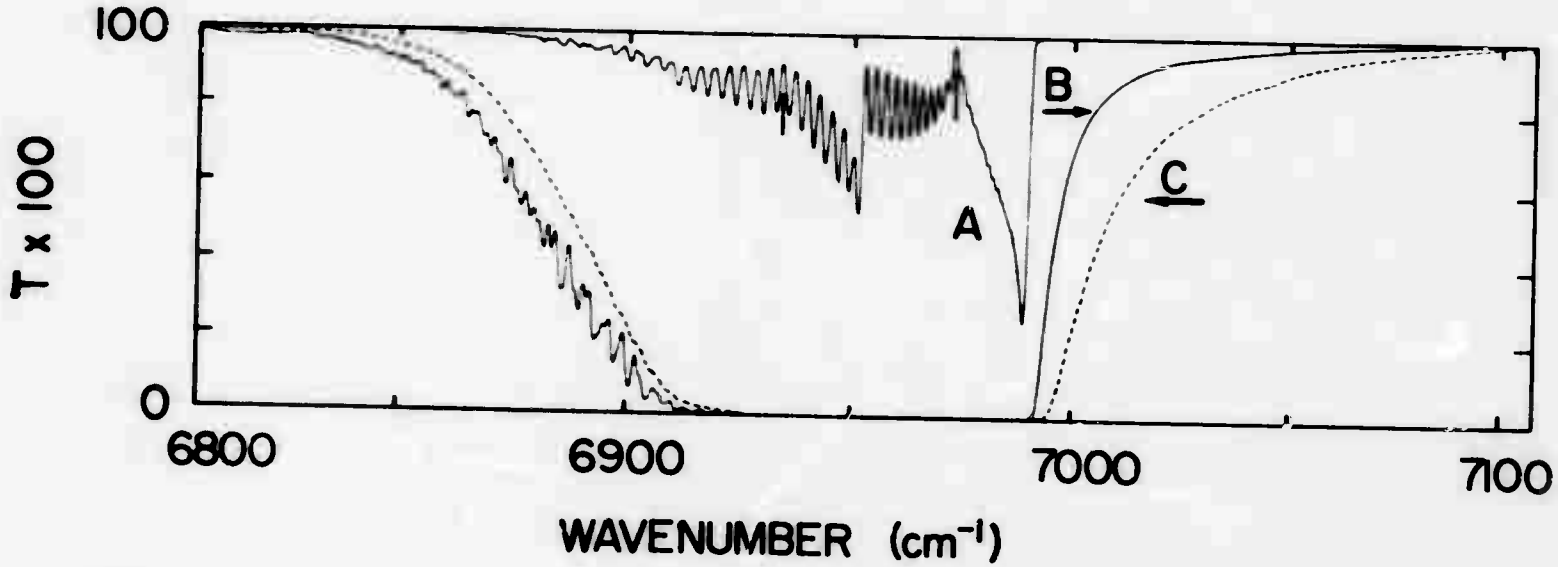

FIG. 1. Representative spectral curves in the 7000 cm^{-1} region. The curves were obtained with approximately 1 cm^{-1} slitwidth and correspond to the following samples of pure CO_2:

Sample	p(atm)	L(meters)	u(atm cm_{STP})
A	0.077	469	3,320
B	2.00	469	87,100
C	14.6	32.9	47,300

of B is considerably larger. However, above the band head, the absorption coefficient is due to the extreme wings of the lines and is proportional to pressure. Therefore, in this region Sample C absorbs more than the lower pressure Sample B, although B has the larger absorber thickness. On the basis of the equations in the previous section, we expect the absorption above the band head to be a function of the product (up). In contrast to this, in regions where most of the absorption is due to nearby lines, it is nearly independent of p for constant u when p is sufficiently high to broaden the lines and smooth-out the structure. Therefore, as seen in Fig. 1, the increase in p and decrease in u shift the center of absorption, although the centers and strengths of all the lines remain fixed.

Figure 2 shows three spectral curves in the region of interest near 3800 cm^{-1}. Of primary interest is the contribution to the absorption above 3760 cm^{-1} by the lines which occur below this wavenumber. It is apparent from the structure in the curves that several weak bands occur in the region where the absorption by the extreme wings of the distant lines is being measured. In order to determine the quantities of interest, we attempted to account for the absorption by the weak, nearby bands; the broken curves represent the transmittance that we would expect if the weak bands were not present. In accounting for the nearby lines we investigated samples covering a wide range of pressures and made use of the difference in the pressure dependence of the contributions by the nearby lines and by the distant lines.

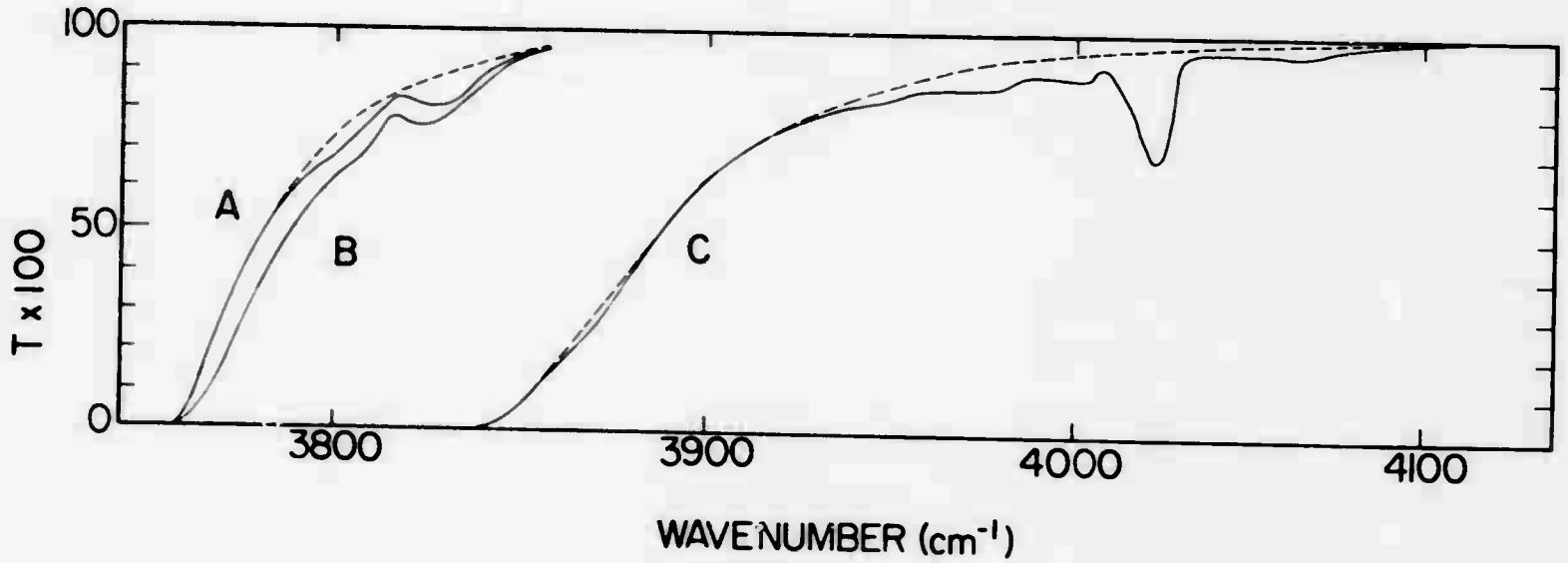

FIG. 2. Representative spectral curves in the 3800 cm^{-1} region. The curves were obtained with approximately 0.9 cm^{-1} slitwidth and correspond to the following samples:

Sample	p(atm)	P(atm)	Broadening Gas	L(meters)	u(atm cm_{STP})
A	3.04	14.6	He	8.26	2,350
B	3.04	14.6	N_2	8.26	2,350
C	14.6	14.6	pure CO_2	32.9	47,300

The broken portions of Curves A and C indicate the estimated contribution of the strong, distant lines after accounting for the weak, nearby lines.

Absorption by pressure-induced bands exhibit the same pressure dependence as absorption by extreme wings of lines. Therefore, it is more difficult to determine the contribution by pressure-induced bands such as the $22^0 0$ band for which there is evidence between 4040 and 4100 cm^{-1} in Curve C of Fig. 2. The broken portion of this curve represents our best estimate of the transmittance without the influence of the pressure-induced band. It seems unlikely that the contribution by the pressure-induced band is significantly less than we have estimated; it may be an even larger part of the absorption observed in this region. Therefore, the absorption attributed to the extreme wings of the distant lines probably represents a maximum; it seems unlikely that it is significantly more than our estimate.

Table 1 contains a listing of the absorption bands of interest in the three spectral regions studied. Part A provides information about the bands which occur below the band heads and contain the lines whose shapes are studied. Part B contains information about the relatively weak bands which occur in the spectral regions where the absorption coefficient is measured. Contributions by these bands are accounted for in order to determine the contribution due to the bands listed in Part A.

Curves A and B in Fig. 2 represent two samples with the same CO_2 pressure and the same path length. Helium has been added to the CO_2 in Sample A to produce a total pressure of 14.6 atm while Sample B contains enough N_2 to produce the same total pressure. Since Curve B falls below Curve A, it is apparent that N_2 is more effective than He as a foreign-

TABLE 1

IDENTIFICATION, POSITIONS, AND STRENGTHS OF BANDS

Part A - provides information about the bands containing the lines whose shapes are studied.

Part B - contains information about the relatively weak bands which occur in the spectral regions where the absorption coefficient is measured. The contributions by these bands are subtracted from the observed absorption to determine the contribution due to the bands listed in Part A.

Part A

BAND[a] IDENTIFICATION	BAND[b] CENTER (cm^{-1})	STRENGTH ($atm^{-1}cm^{-1}$ $_{STP}$ cm^{-1})	REMARKS
		7000 cm^{-1} Region (1.4 μ)	
$01^{1}3\text{-}01^{1}0$	6935.05 C	0.0033 0.0083 at 431°K	
$00^{0}3$	6972.49 C	0.041 0.039 at 431°K	Band head at R40, 6988.56 cm^{-1}. Strongest line, R16, at 6982.94 cm^{-1}
		3800 cm^{-1} Region (2.7 μ)	
$03^{1}1\text{-}01^{1}0$	3680.30 C	2.3	
$02^{0}1$	3612.81 C	29.0	
$10^{0}1$	3714.76 C	44.9	Strongest line, R16, at 3727.10 cm^{-1}
$11^{1}1\text{-}01^{1}0$	3723.21 C	3.5	
		2400 cm^{-1} Region (4.3 μ)	
$01^{1}1\text{-}01^{1}0$	2336.7	210	
$00^{0}1$	2349.3	2700	Band head at R122, 2397.1 cm^{-1}. Strongest line, R16, at 2361.5 cm^{-1}

TABLE 1 (Continued)

IDENTIFICATION, POSITIONS, AND STRENGTHS OF BANDS

Part B

BAND[a] IDENTIFICATION	BAND[b] CENTER (cm^{-1})	REMARKS
	7000 cm^{-1} Region (1.4 μ)	
		No absorption lines were observed between band head and 7100 cm^{-1}.
	3800 cm^{-1} Region (2.7 μ)	
$20^{0}1 \leftarrow 02^{0}0$	3814.26 C	
$14^{0}0$	3856.72	
$01^{1}2 \leftarrow 02^{2}0$	3980.6	
$00^{0}2 \leftarrow 01^{1}0$	4005.9	
$22^{0}0$ PI	4064.0	Evidence in Curve C, Fig. 2.
	2400 cm^{-1} Region (4.3 μ)	
$04^{0}0$ (18)	2500.4	(18) bands are prominent in Fig. 3.
$12^{0}0$ (18)	2614.2	
$20^{0}0$ (18)	2757.0	
$04^{0}0$ (17)	2524.2	(17) bands are expected to be very weak and overlapped by stronger bands. Possible evidence of 20 0 (17) band in Curve B, Fig. 3.
$12^{0}0$ (17)	2641.1	
$20^{0}0$ (17)	2775.4	
$04^{0}0$ PI	2543.3	Not observable.
$04^{2}0$ PI	2585.1	Probably obscured by 12 0 (18) band.
$12^{0}0$ PI	2670.9	Evidence in Curve B, Fig. 3.
$12^{2}0$ PI	2760.7	Probably obscured by 20 0 (18) band.
$20^{0}0$ PI	2797.0	Probably obscured by 12 0 (18) band.

[a]Lower level is $00^{0}0$ unless indicated otherwise. (17) and (18) refer to $C^{12}O^{16}O^{17}$ and $C^{12}O^{16}O^{18}$ molecules; other bands are $C^{12}O_2^{16}$. PI denotes a pressure-induced band.

[b]Values followed by C are from Courtoy; all others are calculated from energy levels given by Stull, Wyatt, and Plass.

broadening gas. Since the bands between 3600 and 3800 cm^{-1} are considerably stronger than those studied in the 7000 cm^{-1} region, we have been able to measure the absorptance much farther from the centers of the absorbing lines than in the higher-wavenumber region.

The 2400 cm^{-1} region is shown in Fig. 3. The continuum portion of the absorption above the band head near 2400 cm^{-1} is mostly due to the very strong $00^{0}1$ band whose center occurs at 2349.2 cm^{-1}. Most of the structure above 2400 cm^{-1} is due to three bands of $C^{12}O^{16}O^{18}$ which arise from transitions that are forbidden in the symmetric $C^{12}O_2^{16}$ molecule. However, these transitions are allowed in the isotopic molecule because of the asymmetry introduced by the presence of the O^{18} atom. The corresponding bands of $C^{12}O^{16}O^{17}$ are much weaker since the asymmetry of the molecule is less and the abundance of the O^{17} atom is only approximately one-fifth that of O^{18}. The contribution by the isotopic bands as well as a few pressure-induced bands above 2400 cm^{-1} were accounted for in order to determine the absorption by the extreme wings of the strong lines whose centers occur below 2400 cm^{-1}.

The strength of the $00^{0}1$ band near 2400 cm^{-1} was taken from WSB;[4] their value is also in good agreement with the results of other workers. Strengths of the bands listed in Part A of Table 1 for the 3800 cm^{-1} and 7000 cm^{-1} regions were determined from spectral curves of samples at approximately 15 atm. At this pressure the spectral lines are sufficiently broadened that the structure within the band is smoothed out, and the transmittance measured with the spectrometer closely approximates the

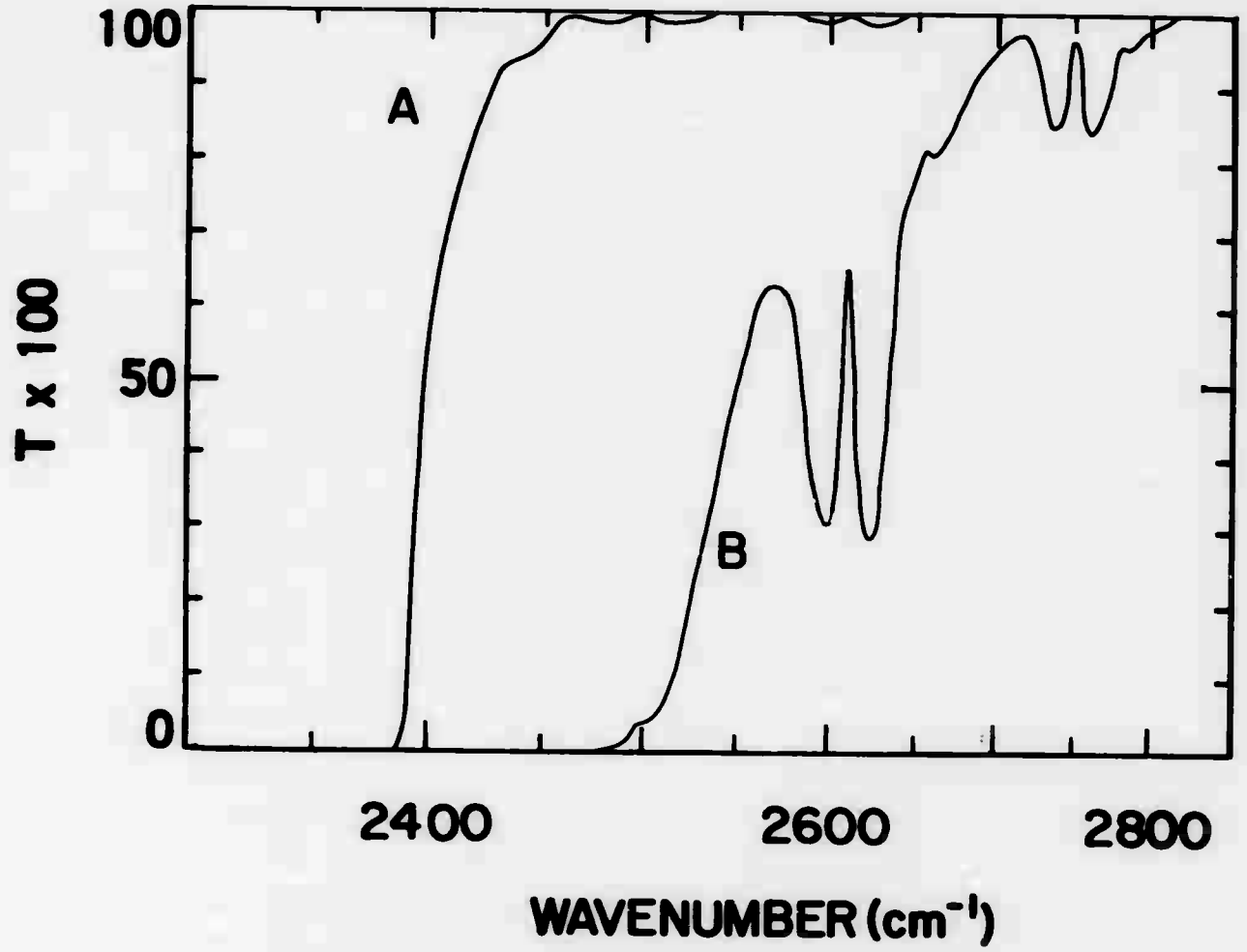

FIG. 3. Representative spectral curves in the 2400 cm^{-1} region. The curves were obtained with approximately 2.5 cm^{-1} slitwidth and correspond to the following samples of pure CO_2:

Sample	p(atm)	L(meters)	u(atm cm_{STP})
A	0.0353	469	1,530
B	0.976	933	84,400

true transmittance. Methods described previously[8] were used to determine the strengths of each of the separate bands in regions of overlapping. Strengths of individual lines were calculated from the band strengths by use of the appropriate theoretical expressions.[6,7]

The half-widths, α_s^o, of self-broadened CO_2 lines at 1 atm were assumed to vary with quantum number J according to Fig. 4, which is based on empirical equations derived by WSB[4] from 15 μ CO_2 data obtained by Madden.[9] In order to check the validity of Fig. 4, we have used the curve-of-growth technique to measure the half-widths of several CO_2 lines in various regions of the spectrum for values of J less than approximately 25. Our results are generally in good agreement with the curves shown in Fig. 4. No significant difference in the half-widths of the lines having the same J value for different bands has been observed. We will show later that our results on shapes of the extreme wings of the lines are not influenced strongly by modifications in the relationship between α_s^o and J, particularly for large J.

The ratios, α_b^o/α_s^o, of the half-widths of foreign-broadened lines to those of self-broadened lines are given in Table 2. The ratios for H_2 and N_2 have been determined as part of the present investigation. The results for A, He, and O_2 are based on the present N_2 measurements and ratios given by Burch, Singleton, and Williams[10] for N_2 broadening and broadening by these gases. Results of quick checks of the relative broadening abilities agree well with those of BSW. No significant differences in the ratios for a given gas have been observed in the three different spectral regions.

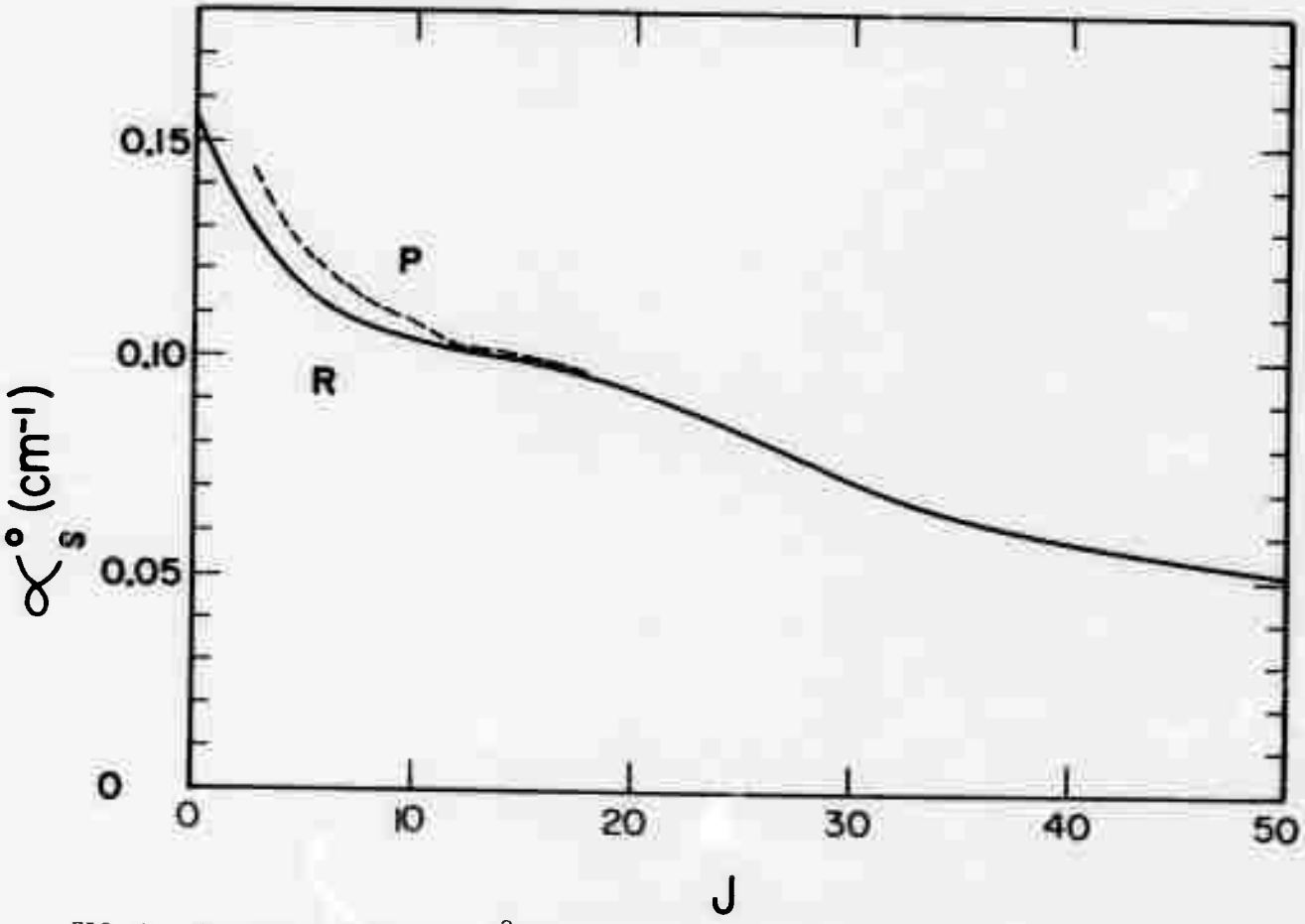

FIG. 4. Normalized half-width γ_s^o of self-broadened CO_2 lines at 1 atm plotted versus J. The curves for the two branches are based on the following empirical equation, which was derived by Winters, Silverman, and Benedict[4] and from data obtained by Madden.[6]

$$\gamma_s^o(\mathrm{cm}^{-1}) = 0.050 + 0.12 \exp[-0.16|m|] + 0.0042|m| \exp\left[-\frac{B''m(m-1)}{kT}\right],$$

where $m = J + 1$, in the R-branch, and $m = -J$ in the P-branch. This equation is applicable for $J \leq 50$; for $J > 50$, we assumed $\gamma_s^o = 0.05\ \mathrm{cm}^{-1}$.

TABLE 2

RELATIVE HALF-WIDTHS OF CO_2 LINES BROADENED BY VARIOUS GASES

Broadening Gas	$\gamma_s^o / \gamma_{CO_2}^o$
CO_2	1.00
N_2	0.83
A	0.65
He	0.49
O_2	0.68
H_2	1.17

Figure 5 contains portions of four spectral curves which illustrate the technique used to determine the ratio of foreign broadening to self broadening. Curve A represents a sample of pure CO_2 with the pressure and path length indicated. After obtaining Curve A, the path length of the multiple-pass absorption cell was changed to approximately four times its original length, and the CO_2 pressure was adjusted to provide the same absorber thickness as for Sample A. Nitrogen was then added to the sample, and spectral curves B, C, and D were scanned with the sample at the total pressures indicated. We note that Curves A and C are nearly coincident near the centers of the lines, while D approximates A near the transmittance maxima between the lines. Since the spectral slitwidths and absorber thicknesses are the same for all the samples, we conclude that the shapes of the N_2-broadened lines are different from those of the self-broadened lines as close as 0.5 cm^{-1} to the line centers. (Two lines are said to have the same shape if $f(\ell, \nu-\nu_o)$ (Eq. (3)) is the same at all $(\nu-\nu_o)$ when the pressures are adjusted so that the half-widths are equal.) The results discussed in following sections make it clear that N_2-broadened lines have quite different shapes from self-broadened lines when $(\nu-\nu_o)$ is more than a few cm^{-1}; however, the method used to obtain those results is not applicable for $(\nu-\nu_o)$ less than approximately 3 cm^{-1}. Therefore, the method indicated by Fig. 5 can provide additional information about the shapes of lines nearer their centers. Because of the finite spectral slitwidth of the spectrometer, the true shapes of the lines cannot be determined near the centers where the transmittance changes rapidly with wavenumber.

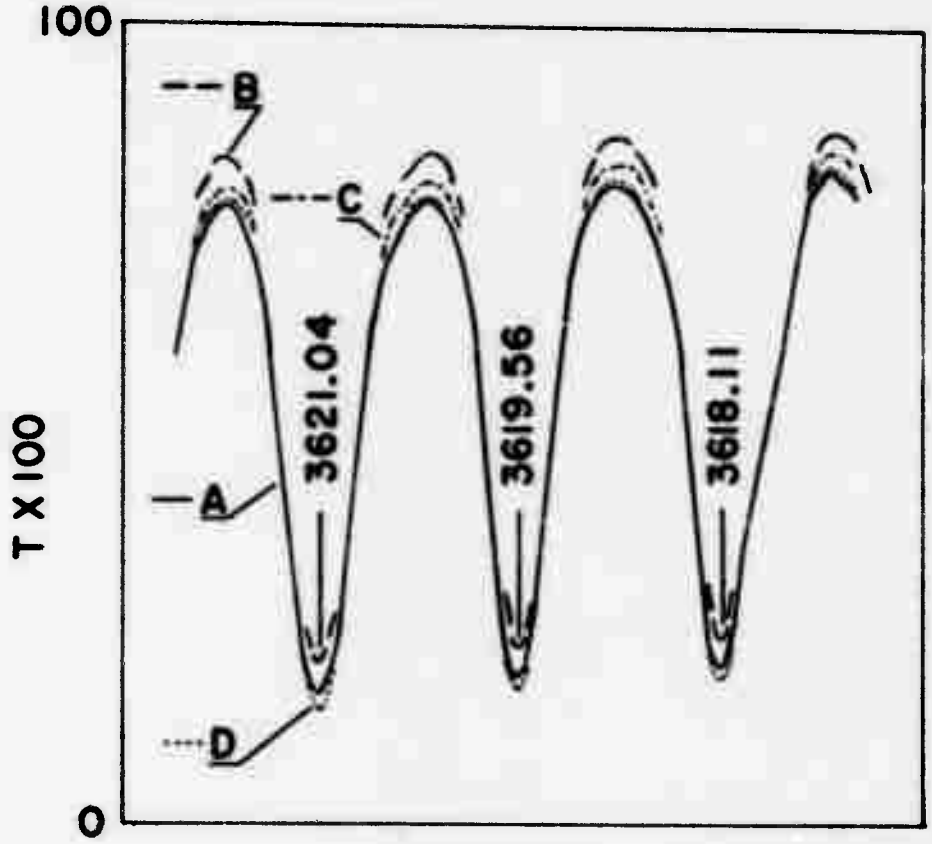

FIG. 3. Spectral curves showing comparison of self-broadened and N_2-broadened lines. All four samples represented by the curves have the same absorber thickness, and all curves were scanned with the same spectral slitwidth. Sample A is composed of pure CO_2, while samples B, C, and D contain CO_2 - N_2. The sample parameters are:

Sample	p(atm)	P(atm)	L(meters)
A	0.0527	0.0527	0.16
B	0.0111	0.0527	12.8
C	0.0333	0.0999	12.8
D	0.0556	0.0556	12.8

the presence of N_2 is more effective to broaden the absorption by the pure CO_2 sample at points in greater between the lines than near the line centers. The [illegible] in the line centers are identical.

Since the half-widths of the lines shown in Fig. 5 are considerably less than the spectral slitwidth of the spectrometer, we cannot determine the half-widths directly from the curves. However, we can determine the ratio $\alpha^o_{N_2}/\alpha^o_s$ if we assume that the shapes of the N_2-broadened and self-broadened lines are similar over a region near their centers that is comparable to the spectral slitwidth. Since Curve C nearly matches Curve A near the line centers, we assume that the half-widths of the lines are the same for the corresponding samples since the absorber thicknesses and spectral slitwidths are identical. Therefore, $\alpha^o_{N_2}/\alpha^o_s$ can be determined by use of the following equation:

$$p^{(A)} = p^{(C)} + p^{(C)}_{N_2} \alpha^o_{N_2}/\alpha^o_s, \tag{12}$$

where the superscripts (A) and (C) refer to the corresponding samples, and p and p_{N_2} are the CO_2 and N_2 pressures, respectively. By substituting the appropriate pressures into Eq. (12) for several sets of measurements, we have determined that $\alpha^o_{N_2}/\alpha^o_s = 0.83 \pm 0.06$. This value compares favorably with 0.75 ± 0.04 obtained by Patty, Manning, and Gardner[11] with a CO_2 laser as a radiation source. The measurements of Patty et al represent the absorption at the center of the P20 line of the 10^00-00^01 band. Since our value represents an average over the region within 0.2 - 0.3 cm^{-1} of the center, any difference in the shapes of the N_2-broadened and self-broadened lines within this interval would produce a difference between our results and those of Patty et al.

From the portions of the curves between the lines, we can show that N_2 broadening is only approximately 0.77 times as effective as self broadening; i.e., the absorption coefficients are identical when the pressure of a pure CO_2 sample is 0.77 times the pressure of a very dilute mixture of CO_2 in N_2. This is approximately 7% less than the value 0.83 obtained near the line centers. Although this difference is small, we believe it is significant since results consistent with Fig. 5 were observed in different spectral regions and for a variety of samples. Burch, Singleton, and Williams[10] have measured the ratio of N_2 broadening to self broadening of CO_2 lines with a spectrometer having low enough resolution that the individual lines were not resolved. Since most of their samples produced considerable absorption, they were nearly opaque near the line centers and most of the increase in absorptance due to increasing pressure occurred near the absorptance minima between the lines. It is, therefore, not surprising that their value, 0.77 ± 0.05, for the ratio of the broadening abilities agrees with the 0.77 obtained in the present investigation for the regions near the absorptance minima.

NORMALIZED ABSORPTION COEFFICIENTS

Curves of the normalized absorption coefficients have been obtained for several broadening gases by substituting into Eq. (11) values of transmittance from curves which represent samples covering very wide ranges of absorber thickness and pressure. Figure 6 shows K_s^o, the normalized absorption coefficient for CO_2 self broadening in the 7000 cm^{-1} region. The solid curve represents the experimental results, and the various geometrical symbols represent data from samples at different pressures. We note that throughout the region from 7010 to 7060 cm^{-1} there is very good agreement between results obtained from samples whose pressures vary from less than 2 atm to approximately 15 atm. This result confirms the assumption that the absorption coefficient is proportional to pressure when $(\nu-\nu_o) \gg$ [illegible] as indicated by Eqs. (10) and (11).

The upper curve in Fig. 6 represents values of K_s^o calculated by assuming that all of the lines have the Lorentz line shape. The lower

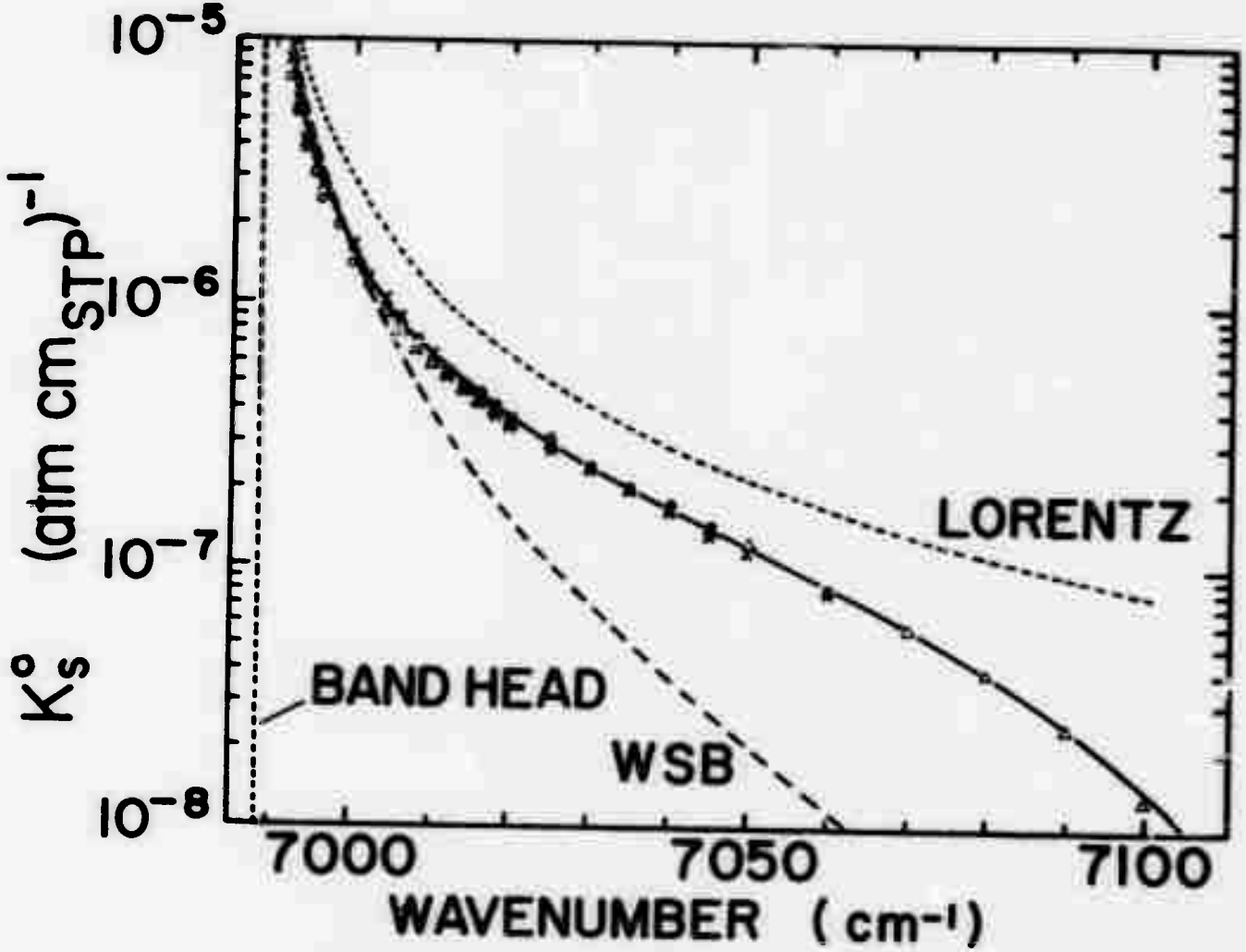

FIG. 6. K_s^o versus ν for CO_2 self broadening between 6900 and 7100 cm^{-1}. The various geometrical figures on the solid curve correspond to samples having the following total pressures: $x \leq 2$ atm; o ~ 8-10 atm; Δ ~ 15 atm. The LORENTZ curve represents the absorption coefficient calculated by assuming the lines have the Lorentz shape. The WSB curve represents calculated results based on the line shape found by Winters, Silverman, and Benedict[4] for the $00^0 1$ band near 2400 cm^{-1}. The position of the band head is indicated.

curve represents calculated values based on the modified line shape derived by WSB[4] from absorption measurements in the 2400 cm^{-1} region (4.3 μ band). It is apparent from these curves that the absorption lines in the 7000 cm^{-1} region are sub-Lorentzian, but their wings are considerably stronger than the lines in the 2400 cm^{-1} region. The shapes of the absorption lines in the different spectral regions are compared in more detail below.

Figure 7 shows similar results for broadening by He and N_2 with a portion of the CO_2 curve from the previous figure repeated for comparison. We note that at 7010 cm^{-1}, K^o is only approximately one-tenth as great for N_2 as for self broadening. From this result it is apparent that the absorption by the wings of N_2-broadened lines is much less than that by self-broadened lines. We also see that the wings of the He-broadened lines are even less absorbing than N_2-broadened ones. Since K^o_{He} and $K^o_{N_2}$ are so small, we were able to measure these quantities only over the spectral regions indicated.

A few measurements on broadening by A, O_2, and H_2 were also made in this region. Upon reducing the data, we found that the results were not as consistent as those for N_2 and He; therefore, they have not been included in Fig. 7. However, values of $K^o_{H_2}$ agreed to within 30 or 40 percent with corresponding values of K^o_{He}. Similarly, values for A and O_2 apparently agree with those for N_2 to within approximately the same accuracy. Broadening by A, O_2, and H_2 in other spectral regions is discussed below.

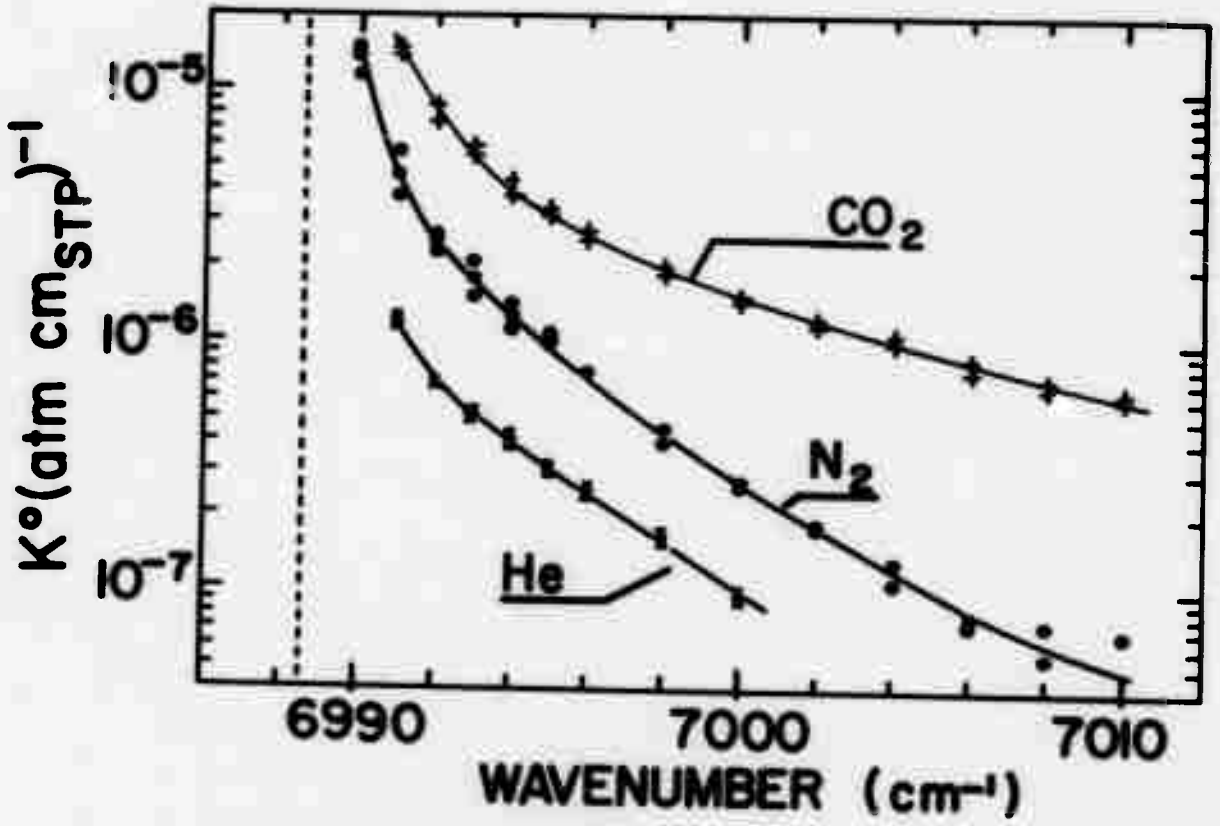

FIG. 7. K^o for N_2, He, and self broadening between 6990 and 7010 cm^{-1}. A portion of the curve for self broadening in Fig. 6 is repeated for comparison. The vertical dashed line indicates the position of the band head.

Figure 8 shows the results for self broadening and N_2 broadening in the 3800 cm^{-1} region. We recall from Fig. 2 that several weak bands in the region of interest had to be accounted for before we could determine the contribution by the lines below 3760 cm^{-1}. Reliable measurements were limited to wavenumbers where the contribution by the weak, nearby bands was considerably smaller than that by the distant lines. We have assumed that K^o can be represented by a smooth curve drawn through the data points. As pointed out in the discussion of Fig. 2 the portion of the absorptance between approximately 4000 and 4100 cm^{-1} that we have attributed to the extreme wings of the strong lines probably represents a maximum. Therefore, the curve in Fig. 8 also is believed to represent maximum values throughout the same region. Values of $K^o_{N_2}$ could not be determined above 3900 cm^{-1} since the additional absorptance due to increasing the N_2 pressure in CO_2 + N_2 mixtures was too small to measure.

Plots of K^o versus ν in the 3800 cm^{-1} region are shown for various broadening gases in Fig. 9. The curves corresponding to N_2, O_2, and A are close to each other near the band head, as they are near 7000 cm^{-1}. Also, as in the 7000 cm^{-1} region, values represented by the He curve are only approximately one-tenth those represented by the self-broadening curve. Data on H_2 broadening are limited to the region between 3770 and 3780 cm^{-1} where the absorption by the CO_2 lines is large compared to the absorption by an H_2 pressure-induced band. At higher wavenumbers the absorption by the H_2 band is too large to be accounted for accurately.

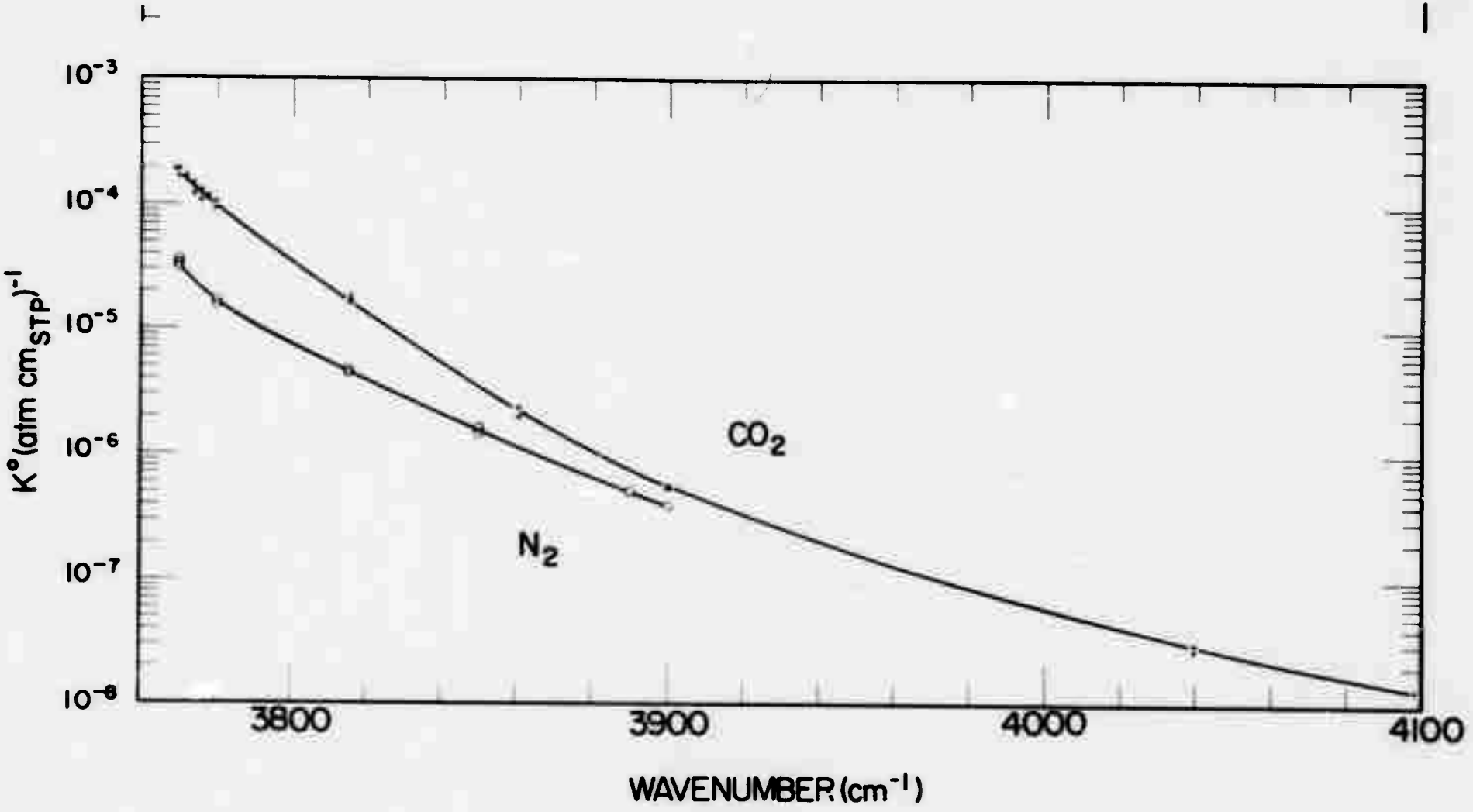

FIG. 8. K^o for self and N_2 broadening between 3770 and 4100 cm^{-1}. The curves represent the contribution due to the lines below 3780 cm^{-1}; the contribution of the lines between 3780 and 4100 cm^{-1} has been subtracted from the observed absorption coefficient. The curves are based on data points at wavenumbers where the absorption by nearby lines is small. Because of possible errors in the corrections made, the uncertainty in the curve is large above 3900 cm^{-1}.

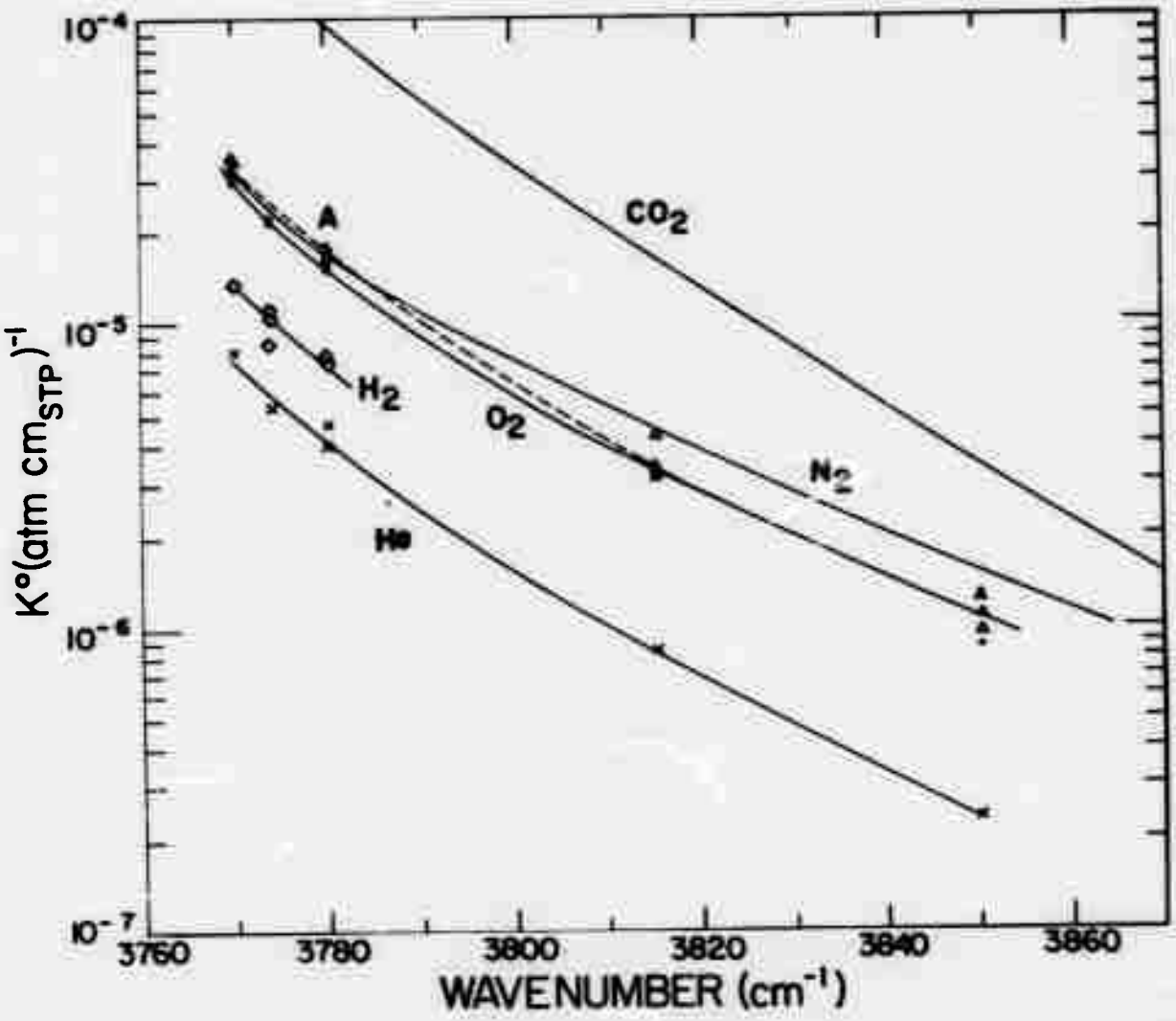

FIG. 9. K^o for various gases between 3770 and 3860 cm^{-1}. Portions of the CO_2 and N_2 curves in Fig. 8 have been included for comparison. Data on H_2 broadening are limited to a short region where the absorption by CO_2 lines is much greater than that by H_2 absorption. The O_2 and A curves are essentially coincident between 3815 and 3850 cm^{-1}.

Figure 10 contains the curves of K^o in the 2400 cm^{-1} region for CO_2, N_2, and A. As in the 3800 cm^{-1} region, the N_2 and A curves are nearly coincident near the band head. However, at higher wavenumbers, these two curves diverge, with the N_2 curve occurring above the one corresponding to A. Also, as in the 3800 cm^{-1} region, the N_2 curve approaches the CO_2 curve when the distance from the edge of the absorption band is approximately 100-150 cm^{-1}. The portion of the absorption due to the nearby bands is too large to be accounted for accurately above 2570 cm^{-1}. However, from Curve B of Fig. 3, we can set upper limits on K_s^o of approximately 5×10^{-8} $(atm\ cm_{STP})^{-1}$ at 2710 cm^{-1} and 5×10^{-9} $(atm\ cm_{STP})^{-1}$ at 2830 cm^{-1}.

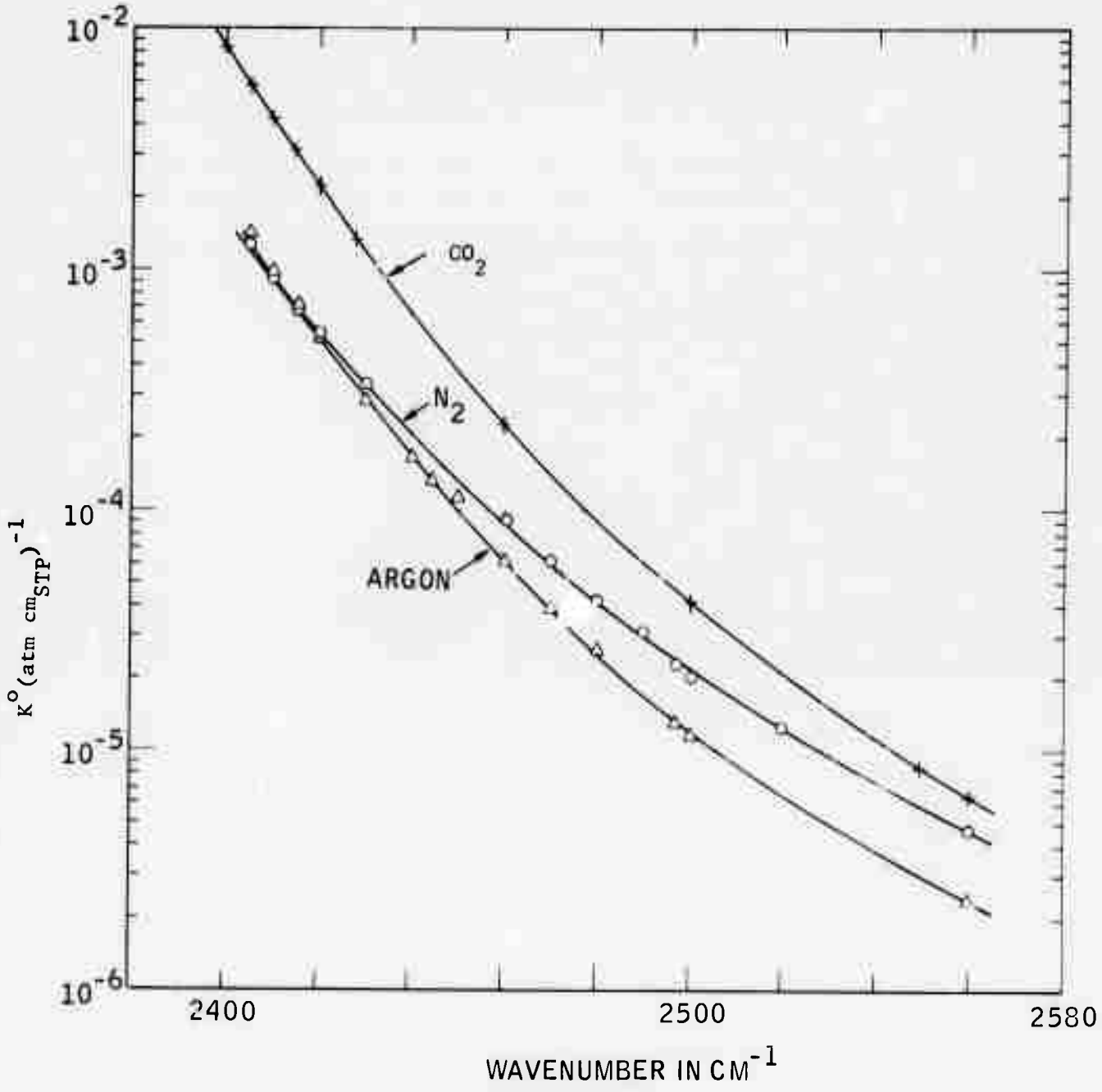

FIG. 10. K^o for CO_2, N_2, and A in the 2400 cm^{-1} region. The curves represent the contribution of lines below 2400 cm^{-1}. Above 2570 cm^{-1} it is difficult to account for the contribution of the nearby bands; however, from Curve B of Fig. 3, we can set upper limits on K_s^o of 5×10^{-8} and 5×10^{-9} (atm cm_{STP}) at 2710 and 2830 cm^{-1}, respectively.

CURVES OF X VS $(\nu-\nu_o)$

Curves of X versus $(\nu-\nu_o)$ for several different broadening gases are shown in Figs. 11-14 for the three different spectral regions investigated. The curves have been derived from experimental values of K^o by the trial-and-error method described previously. In most cases, values of K^o calculated by substituting values from the X curves into Eq. (11) agree with the experimental values of K^o to within two or three percent. Figure 11 shows curves for self broadening in the 7000 cm^{-1} region. Curve A represents samples at room temperature, 296°K, while Curves B and C correspond to samples at 431°K. We had to assume values for the half-widths of the lines at 431°K since this quantity was not measured. Curve B was obtained from the 431°K data by assuming that the half-widths of the self-broadened absorption lines vary inversely with temperature when the pressure is kept constant. Curve C was derived from the same data as Curve B, but the normalized half-widths were assumed to vary inversely as the square-root of the temperature.

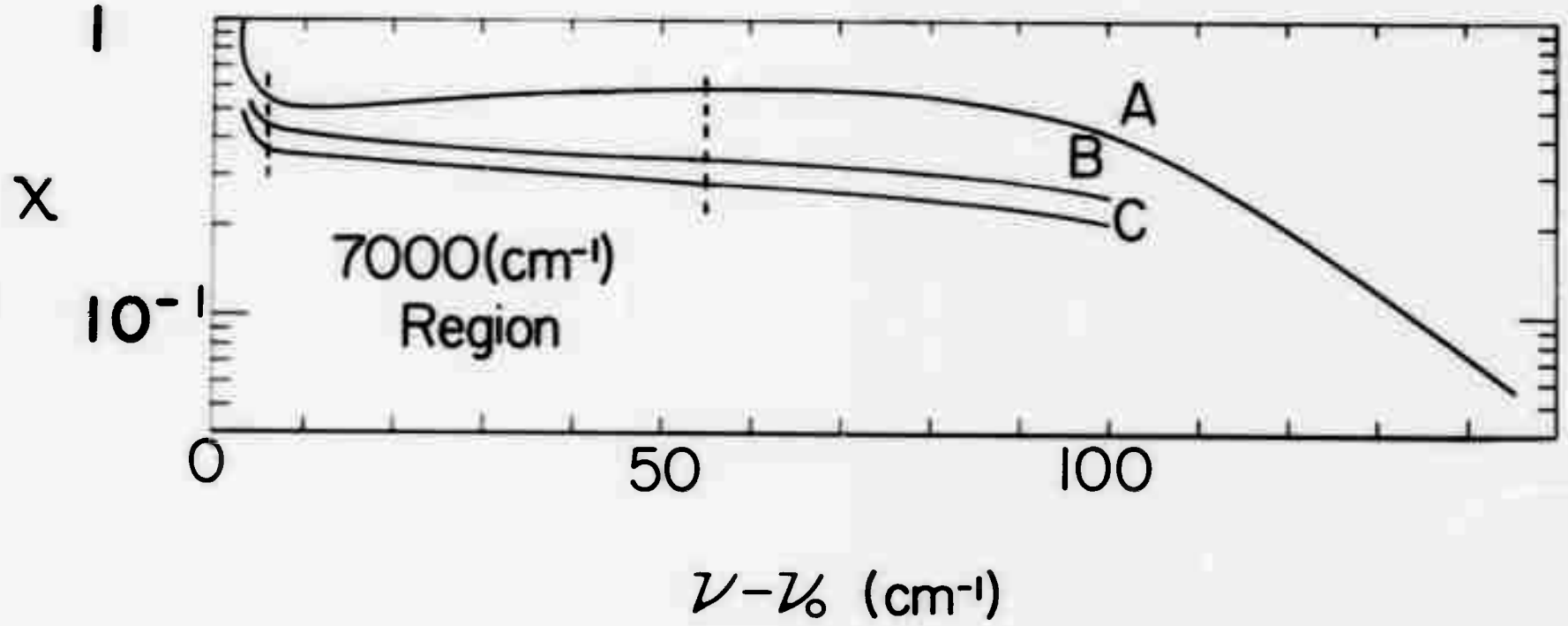

FIG. 11. X for self-broadened CO_2 lines in the 7000 cm^{-1} region. The upper curve corresponds to measurements made at room temperature, 296°K. Curves B and C correspond to 431°K. B is based on the assumption that the half-widths of self-broadened lines vary inversely with absolute temperature when the pressure is maintained constant; C is applicable if the half-widths vary inversely with the square-root of temperature.

Figure 12 shows the curves of X versus $(\nu-\nu_o)$ for broadening by He, CO_2, and N_2 at room temperature and by N_2 at 431°K. Calculated values of K^o are only slightly dependent on the values of X assumed for very small and for large $(\nu-\nu_o)$. Therefore, the uncertainty of the end portions of the curves of X is greater than for the center portion. The regions between the vertical dashed lines in Figs. 11-14 are probably accurate to $\pm$ 10 to 20 percent; outside the interval bounded by the lines, the uncertainty may be considerably greater. Lines in all three spectral regions were assumed to be Lorentzian (X = 1) when $(\nu-\nu_o) > 3$ cm^{-1} for self broadening and when $(\nu-\nu_o) < 0.5$ cm^{-1} for foreign-gas broadening.

Figure 13 contains curves of X versus $(\nu-\nu_o)$ for self broadening and broadening by N_2 and A in the 3800 cm^{-1} region. Since measurements were made over a wider spectral region for pure CO_2 than for mixtures, the CO_2 curve extends to larger $(\nu-\nu_o)$ than do the other curves. We recall that the K^o curve in Fig. 8 is believed to represent maximum values above 3900 cm^{-1}. Since X for $(\nu-\nu_o)$ greater than approximately 200 cm^{-1} is strongly dependent upon K^o for the 3900-4100 cm^{-1} region, the curve of X for $(\nu-\nu_o)$ between 200 and 400 cm^{-1} also probably represents maximum values of this quantity. Figure 14 shows the curves of X for CO_2, N_2, and A for the 2400 cm^{-1} region. The curve for self broadening compares favorably with the analytical expression given by WSB[4] for the same quantity.

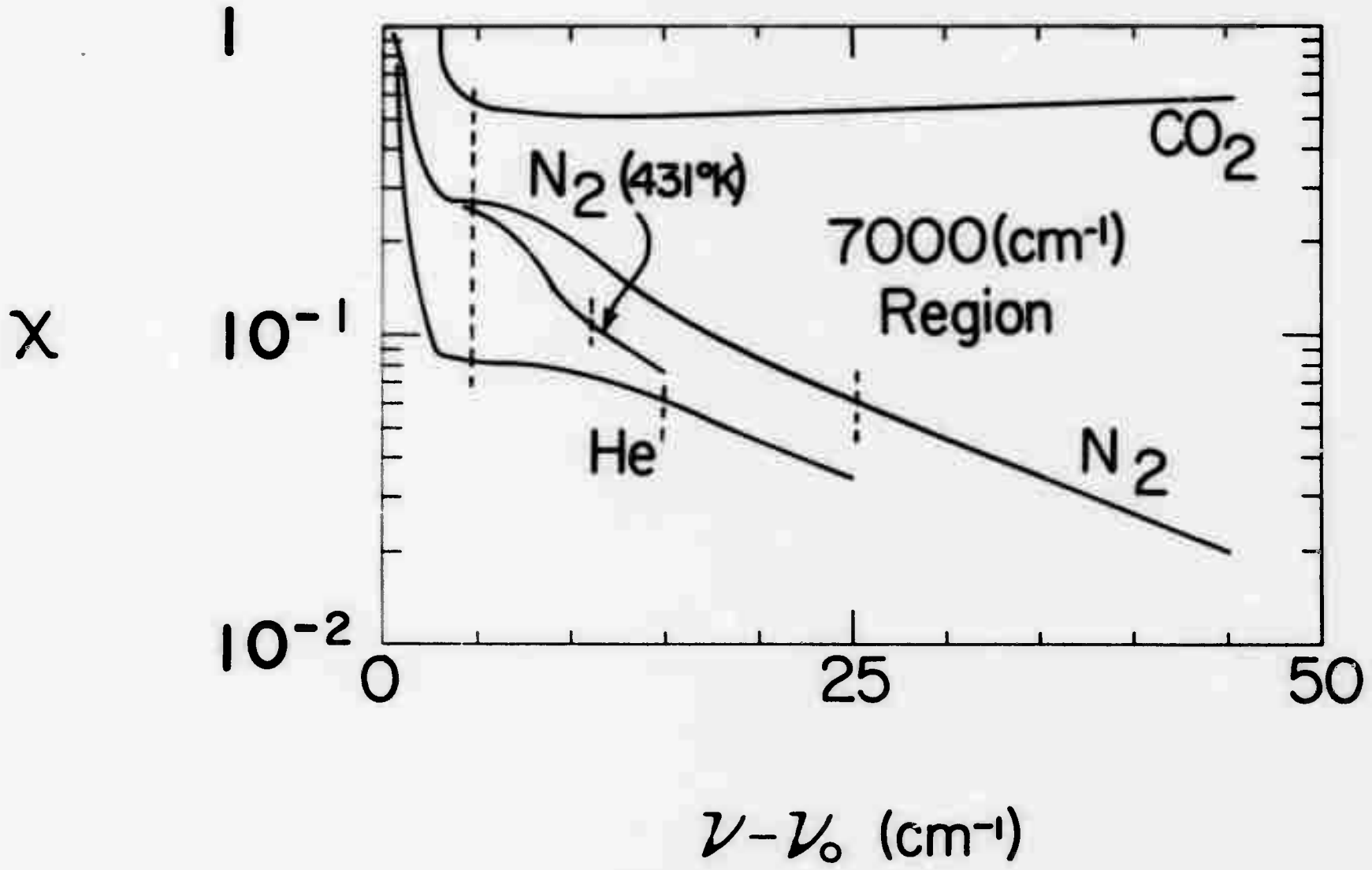

FIG. 12. χ for lines broadened by CO_2, N_2, and He in the 7000 cm^{-1} region. The curve representing N_2 at 431°K is based on the assumption that the normalized half-widths of the lines vary inversely with the square-root of temperature. A portion of the CO_2 curve in Fig. 11 has been included for comparison.

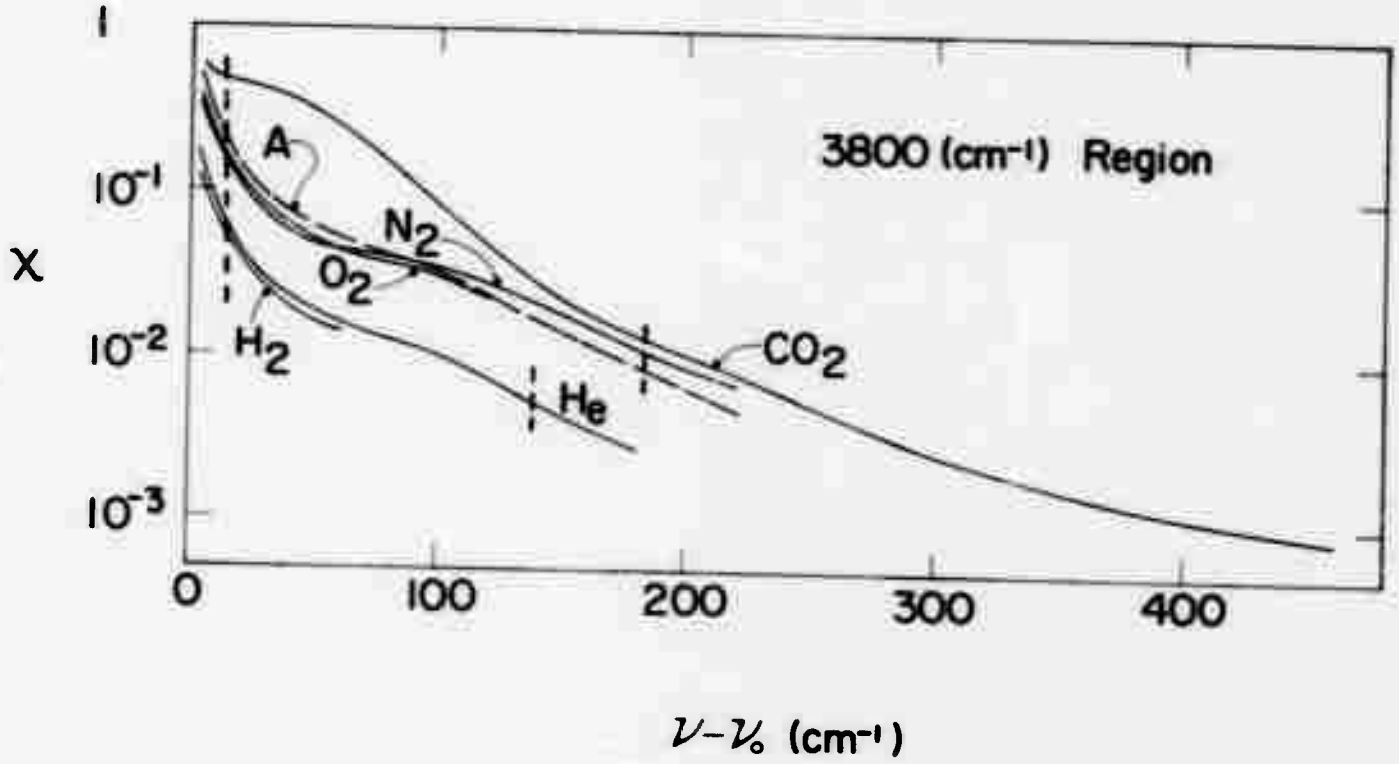

FIG. 13. χ for lines broadened by CO_2, N_2, A, O_2, He, and H_2 in the 3800 cm^{-1} region. For $(\nu-\nu_o) \gtrsim 120$ cm^{-1}, the O_2 and A curves are essentially coincident.

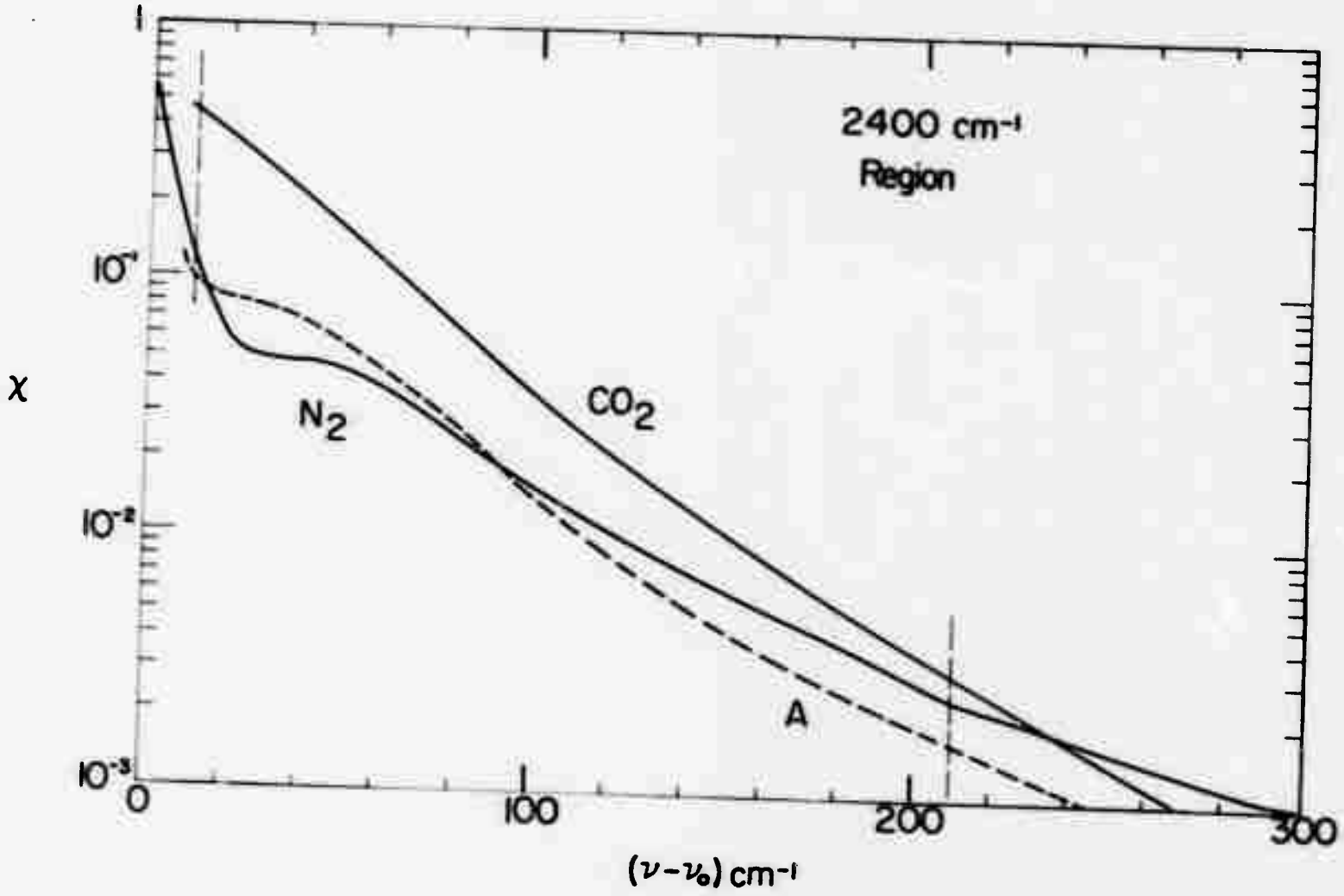

FIG. 14. $\chi(\nu-\nu_0)$ for CO_2, N_2, and A in the 2400 cm^{-1} region.

Before discussing further the results shown in Figs. 11-14, we will consider some of the factors that influence the shapes of these curves. Since all of the curves are based on half-widths given by Fig. 4, it is of interest to determine how the X curves would be changed if we assumed different values for the normalized half-widths of the absorption lines. The solid curves in Fig. 15 are the same as the corresponding curves for self broadening shown in Figs. 11 and 6. The plus signs represent calculated values of K_s^o which are based on values of X given by the upper panel and on line widths from Fig. 4. The squares plotted in the lower panel of Fig. 15 correspond to calculated values of K_s^o based on the solid X curve in the upper panel and on lines whose normalized half-widths, γ_s^o, are 0.092 cm^{-1}, the mean value based on the curves of Fig. 4. We note that the squares deviate significantly from the plus signs only in the region near the band head since a significant part of the absorption near the band head is due to nearby lines whose half-widths were assumed to be approximately 0.060 cm^{-1} when calculating the values represented by plus signs. A good portion of the absorption in this region is also due to the much stronger lines, $J \sim 10$ to $J \sim 20$, which are 4 or 5 cm^{-1} below the band head. However, beyond approximately 15 cm^{-1} from the band head, nearly all of the absorption is due to the stronger lines whose half-widths are approximately the same for both calculations.

The broken portion of the curve in the upper panel of Fig. 15 represents the modification in the X curve that is required to provide agreement with the experimental values of K_s^o if we assume that

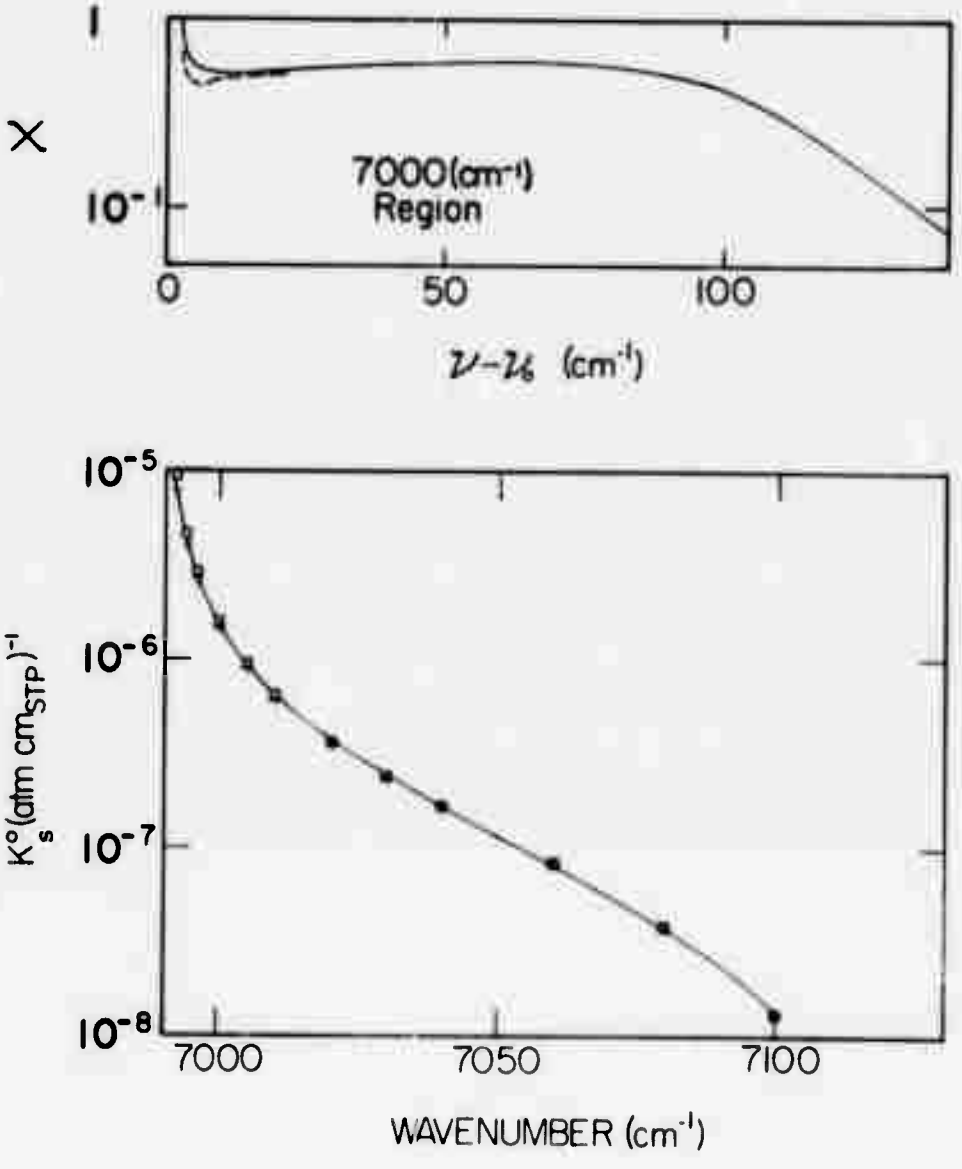

FIG. 15. Influence of assumed line width on calculated curves of $X(\nu-\nu_o)$ and $K_s^o(\nu)$ in the 7000 cm^{-1} region. The curve in the lower panel represents the experimental results for $K_s^o(\ )$. The +'s represent the values calculated on the basis of lines whose X is given by the solid curve in the upper panel and whose half-widths are given by Fig. 4. The □'s represent values calculated on the basis of the same X but with γ^o = 0.092 cm^{-1} for all lines. Values of $K_s^o(\nu)$ based on lines with γ^o = 0.092 cm^{-1} and X modified according to the dashed curve agree with the experimental curve to within ± 2 percent.

$\alpha_s^o = 0.092$ cm^{-1} for all of the lines. The effect on the X curve for other modifications in the values of α_s^o can be inferred from this curve. If all values of α_s^o were increased by 10%, for example, the curve of X would, of course, be shifted down by the same factor.

We see from Table 2 that the band head in the 7000 cm^{-1} region occurs at R40, which is only 5.6 cm^{-1} from R16, the strongest line in the band. By comparison the band head in the 2400 cm^{-1} region occurs at R122 which is more than 35 cm^{-1} from the strongest line. Therefore, many weak lines of high J value contribute significantly to the absorption a few cm^{-1} above the 2397 cm^{-1} band head since they are much closer than the strong lines. Consequently, the shapes of the X curves for the 2400 cm^{-1} region are probably more dependent than the one for the 7000 cm^{-1} region upon the half-widths assumed for high J lines. This is also true for the 3800 cm^{-1} region since the strongest lines are several cm^{-1} from the region where K_s^o has been measured.

The curves in Fig. 16 provide information about the dependence of the calculated values of K^o on γ. Conversely, it also shows the variations introduced in the curves of X by errors or changes in the values of K^o which are being matched. Curve A in the lower panel of Fig. 16 shows the experimentally determined curve of $K_{N_2}^o$, which also appears in Fig. 8 for the 3800 cm^{-1} region. The circles in the lower panel which fit the experimental curve very well represent the values of $K_{N_2}^o$ calculated on the basis of the X curve given by A in the upper panel. Curve B in the upper panel represents a modification of a portion of Curve A for $(\gamma - \gamma_o)$

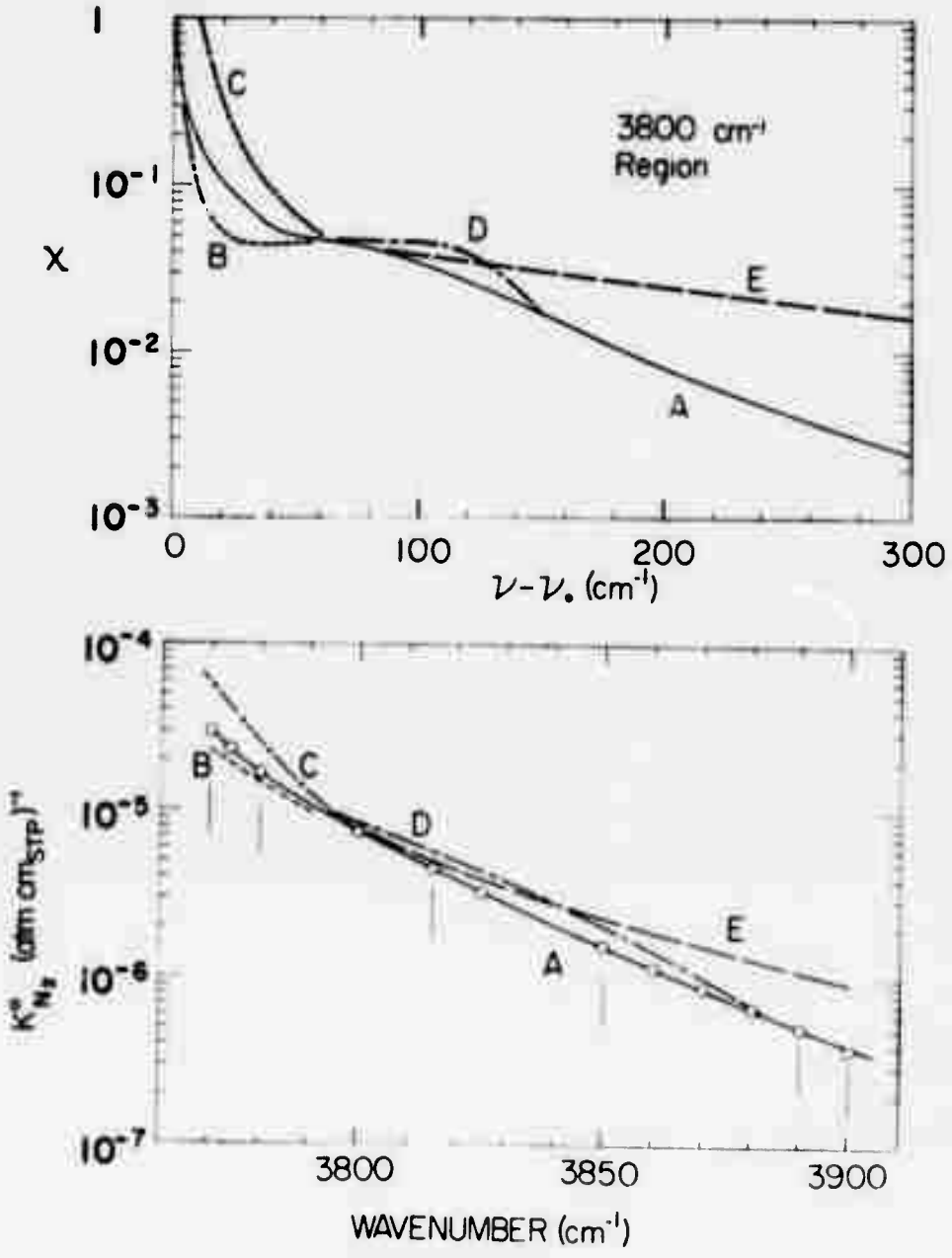

FIG. 16. Curves of χ and $K^o_{N_2}$ showing influence of assumed line shape on the calculated absorption coefficient in the 3800 cm^{-1} region. Curve A in the lower panel represents the experimental results for $K^o_{N_2}$. The circles represent the values calculated on the basis of a line shape whose χ is given by Curve A in the upper panel. Variations in the line shape given by Curves B, C, D, and E in the upper panel were assumed, and the corresponding calculated curves of $K^o_{N_2}$ are shown in the lower panel. The six vertical lines in the lower panel indicate the wavenumbers at which experimental measurements were made.

$< 60\ cm^{-1}$; Curve B in the lower panel represents the resulting calculated values of $K^o_{N_2}$. We see that the modification to the line shape for $(\nu-\nu_o)$ less than 5 and 60 cm^{-1} produces only a relatively small change in the calculated values of $K^o_{N_2}$ between 3770 and 3780 cm^{-1}. From this result we conclude that much of the absorption in this region is due to lines more than 60 cm^{-1} away, although many lines occur within this distance. Above 3800 cm^{-1} the modification represented by Curve B in the upper panel provides no significant change in the $K^o_{N_2}$ curve.

Similarly, the curves marked "C" in both panels of Fig. 16 indicate the influence of a quite different modification to the X curve for $(\nu-\nu_o)$ $< 60\ cm^{-1}$. Of course, modifications B and C do not affect the calculated values of $K^o_{N_2}$ more than 60 cm^{-1} above the highest-wavenumber lines being considered. The rather major change indicated by Curve C provides a sizable change in the calculated values of $K^o_{N_2}$ between 3770 and 3780 cm^{-1} since the relative contribution of the nearby, weak lines is increased. The C curves are based on a Lorentz line shape for $(\nu-\nu_o) \pm 10\ cm^{-1}$ with a sudden decrease in the absorption coefficient as $(\nu-\nu_o)$ increases. The quite significant difference between Curves A and C in the lower panel of Fig. 16 is evidence that N_2-broadened lines are sub-Lorentzian within 10 cm^{-1} of their centers.

The modification represented by Curve D for $60\ cm^{-1} < (\nu-\nu_o) < 150\ cm^{-1}$ is seen to influence the calculated values of $K^o_{N_2}$ from approximately 3790 to 3880 cm^{-1}. We believe that the difference between Curves A and D in the lower panel is less than the uncertainty of the experimental $K^o_{N_2}$

values obtained in this region. Curve E illustrates the effect of quite a large change in X for large $(\nu-\nu_o)$. We see that the calculated values of $K^o_{N_2}$ below 3800 cm^{-1} are not influenced significantly by this modification, indicating that most of the absorption in this region is due to lines within 60 cm^{-1}.

We see from Fig. 16 that errors of 15 or 20 percent in the values of $K^o_{N_2}$ might cause a significant change in the shape of the resulting curve of X, although X at any value of $(\nu-\nu_o)$ might not be changed greatly. For example, if the measured values of $K^o_{N_2}$ fell on Curve B at 3770 and 3780 cm^{-1} and on Curve D at 3815 and 3850 cm^{-1}, the corresponding X curve would fall on Curve B in the upper panel for $(\nu-\nu_o) < 60$ cm^{-1} and on Curve D for $60 < (\nu-\nu_o) < 150$ cm^{-1}. Beyond $(\nu-\nu_o) = 150$ cm^{-1}, the derived curve would fall on the existing Curve A. Thus, relatively small errors in the measurement of $K^o_{N_2}$ may cause quite a difference in the shape of the X curve. Therefore, we must be careful not to place too much significance on the shape of the X curve, although the average value of the curve over relatively wide ranges can be considered reasonably accurate.

We will now return to a discussion of the results shown in Figs. 11-14. In Curve A of Fig. 11, which represents self broadening of CO_2 in the 7000 cm^{-1} region, X appears to reach a minimum when $(\nu-\nu_o) \sim 12$ cm^{-1} and to increase slightly before attaining a maximum at approximately 60 cm^{-1}. In view of the discussion of Fig. 16, we conclude that the minimum near 12 cm^{-1} and the maximum near 60 cm^{-1} may or may not be real. However, it is significant that the average X throughout this region is between 0.5 and 0.6.

According to the simple, classical theory, the half-width of a collision-broadened line is proportional to collision frequency and, therefore, inversely proportional to the square-root of temperature, θ, if the pressure is constant. This $\theta^{-1/2}$ dependence is usually regarded as approximately correct for foreign broadening; however, various experimental and theoretical results indicate that for self-broadening the dependence on temperature may be as strong as θ^{-1}.

Curves B and C of Fig. 11 show the X functions we obtained by assuming a θ^{-1} and $\theta^{-1/2}$ dependence of α_s^o. The influence of temperature on line strengths was accounted for in the calculations. Values on Curve B, which corresponds to a θ^{-1} dependence, are only about 0.6 as large as the room temperature values (Curve A) for the same $(\nu-\nu_o)$. If a weaker temperature dependence is assumed, the deviation from Curve A is even greater. Thus, it is apparent that increasing temperature changes the line shapes with a marked decrease in the extreme wings.

The curve corresponding to N_2 at 431°K in Fig. 12 also falls well below the room temperature curve. The 431°K curve is based on the $\theta^{-1/2}$ dependence of α_s^o. No curve corresponding to the θ^{-1} relationship is shown for N_2 broadening, since this relationship is expected to apply to self broadening only. Because of turbulence in the samples at high pressure and 431°K, we were limited to somewhat smaller samples than at room temperature. Consequently, we could not make reliable measurements as far above the band head at the elevated temperature, and the X curves are limited to smaller $(\nu-\nu_o)$.

A few measurements at elevated temperatures were made in the 3800 cm^{-1} region. However, the absorption by the nearby weak bands increased so rapidly with increasing temperature that the contribution by the extreme wings of the distant lines could not be measured accurately. Most of the lower energy levels involved in the weak bands above 3760 cm^{-1} are excited, so that their populations, and, in turn, the band strengths increase with increasing temperature. However, in spite of the increased absorption by the weak bands, the absorption near 3850 and 3900 cm^{-1} remained approximately constant. From this result we concluded that the absorption by the extreme wings of the strong lines decreased with increasing temperature, as in the 7000 cm^{-1} region.

We note that the N_2 curve in Fig. 12 drops very rapidly to approximately 0.06 at $(\nu-\nu_o) = 25$ cm^{-1}. In accordance with the discussion of Fig. 5, we have assumed that the Lorentz line shape was valid ($\chi = 1$) for N_2 for $(\nu-\nu_o) < 0.5$. Our results do not enable us to determine reliably the curves of χ for $0.5 < (\nu-\nu_o) < 3$ cm^{-1}, and conversely, our calculated values of K^o are relatively insensitive to the values of χ assumed for this region. However, it is apparent from our data that χ is as low as approximately 0.3 for $(\nu-\nu_o) = 5$ cm^{-1}. Although the curve for self broadening is sub-Lorentzian, it does not decrease as quickly as the curve corresponding to N_2 broadening. The He curve decreases even faster than the N_2 curve, reaching approximately 0.08 for $(\nu-\nu_o) = 5$ cm^{-1}. Both the He and N_2 curves appear to have an approximately-level portion after the first sudden decrease, although these level portions do not cover as large

a range of values of $(\nu-\nu_o)$ as does the level portion of the self-broadening curve. Evidence for the large difference between the wings of He- and N_2-broadened lines was mentioned in the discussion of Fig. 2.

As in the 7000 cm^{-1} region, the N_2 curve falls well below the self-broadening curve for the 3800 cm^{-1} region in Fig. 13. However, the two curves tend to approach each other for very large $(\nu-\nu_o)$. This phenomenon was not observable in the 7000 cm^{-1} region, possibly because N_2 measurements could not be made for sufficiently large $(\nu-\nu_o)$. The curves for A, O_2, and N_2 are similar for $(\nu-\nu_o) < 100$ cm^{-1}, but for larger values the N_2 curve falls above the other two. Also, as in the 7000 cm^{-1} region, the He curve falls well below the N_2 curve and is similar to the H_2 curve, which is based on limited data. Thus, H_2, which is a relatively efficient broadener near the line centers (Table 2), is very inefficient for $(\nu-\nu_o)$ more than a few cm^{-1}.

Figure 14 contains similar curves for the 2400 cm^{-1} region. As in the 7000 cm^{-1} the N_2 curve falls considerably below the CO_2 curve then approaches it as $(\nu-\nu_o)$ increases. The apparent crossing of these two curves near $(\nu-\nu_o) = 230$ cm^{-1} may not be significant because of the large uncertainty in the curves near and beyond the crossing point. However, the sudden increase and the gradual decrease in the separation of the CO_2 and N_2 curves is probably significant. The relative shapes of the N_2 and A curves are also similar in the 3800 and 2400 cm^{-1} regions. The A curve lies above the N_2 curve throughout most of the region for $(\nu-\nu_o) < 90$ cm^{-1}, but beyond this point their positions are reversed.

It is of interest that the curves corresponding to the two light molecules, He and H_2, are similar and both are quite different from those representing the heavier molecules. The broadening by these two gases appears to be similar in the extreme wings, although H_2 is a diatomic molecule and He is monatomic. It is apparent from the great divergence of the X curves corresponding to the various gases that the mechanism involved in the broadening of lines several cm^{-1} from their centers is quite different from the mechanism producing the broadening near the centers. The broadening of the extreme wings is more strongly dependent upon the broadening gas.

The results for He and H_2 suggest that broadening in the extreme wings may result from collisions with relatively slow-moving molecules since the number of slow H_2 and He molecules is much less than for heavier molecules at the same temperature. Further support for this suggestion is provided by the decrease in absorption by the wings of the lines as the temperature increases and the number of slow-moving molecules decreases. Of course, there are insufficient data here to prove conclusively that the extreme wings are due to collisions with slow molecules; however, the widely accepted belief that they result from the very hard collisions does not appear to be justified. If broadening in the extreme wings is, in fact, due to slow molecules, the amount of broadening may depend strongly on the amount of time the two colliding molecules remain within a certain distance, rather than on the distance of closest approach.

Argon was investigated since it is monatomic and heavier than either N_2 or O_2. In view of its quite different physical characteristics, it is surprising that its behavior as a broadening gas is so similar to that of O_2. Since the molecular weight of A is approximately the same as that of CO_2, it is apparent that the broadening mechanism in the extreme wings cannot be explained by the molecular weights alone. It is well known[12] that the half-widths of lines depend on the dipole and quadrupole moments of the colliding molecules, so that a knowledge of the masses and shapes of the molecules is not sufficient to predict the broadening characteristics. However, most of the present theories deal with half-widths and shapes near line centers; very little work has dealt with the shapes of the extreme wings.

In order to compare the shapes of the lines in the different spectral regions and to show the line shapes for several different broadening gases, we have constructed the curves in Figs. 17 and 18. The quantity k_{max} is the absorption coefficient at the center of a Lorentz line with $\gamma = 0.1$ cm^{-1}, which is typical of a self-broadened CO_2 line at slightly more than 1 atm. Log-log plots have been used in order to represent the Lorentz shape by a straight line when $(\nu-\nu_o) \gg \gamma$. Each decade has been made twice as long on the abscissa as on the ordinate so that the curves are not as steep as they would be otherwise. Each curve was obtained by multiplying the Lorentz curve by the appropriate value of X from Figs. 11, 13, and 14. Figure 17 shows the ratio k/k_{max} plotted versus $(\nu-\nu_o)$ for self-broadened lines in the three spectral regions indicated. We see that the curves

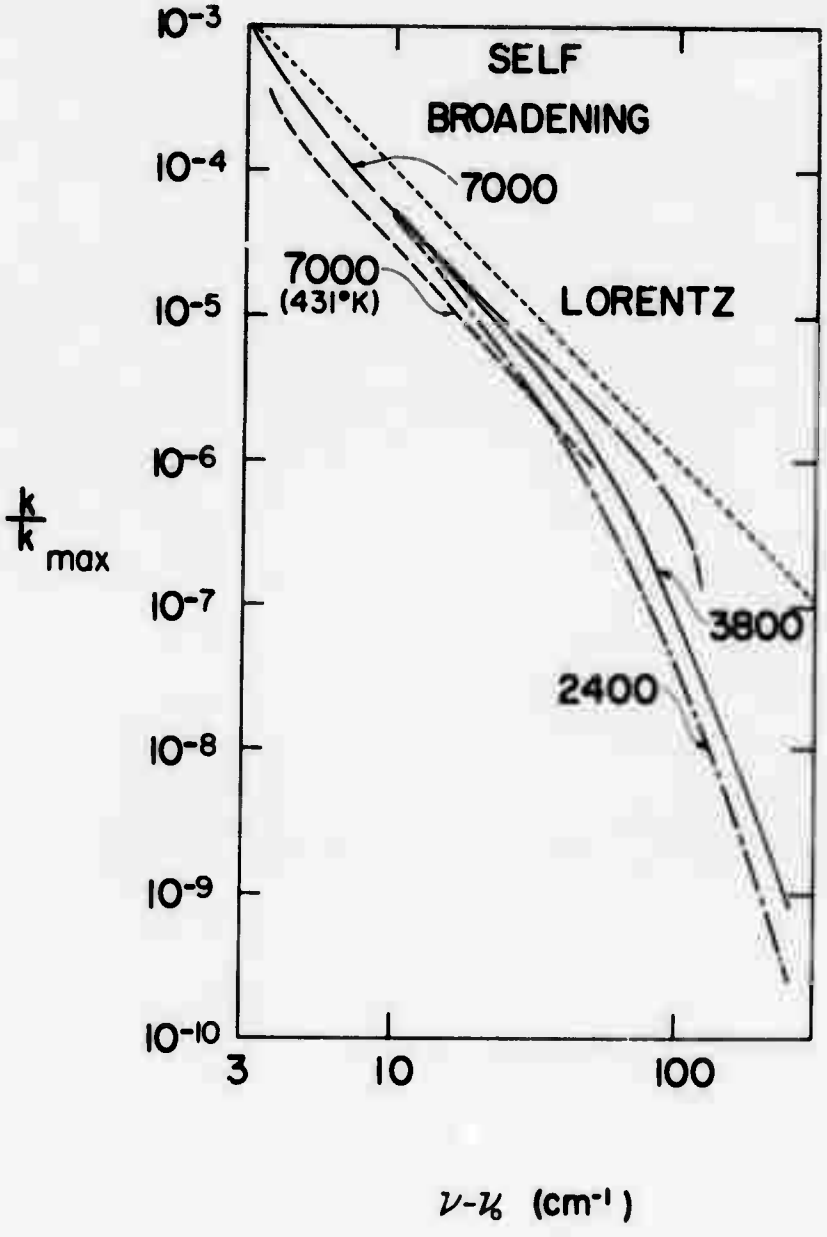

FIG. 17. Ratio k/k_{max} versus $(\nu-\nu_o)$ for self-broadened lines in three spectral regions. The curves correspond to a Lorentz line and to lines in the wavenumber regions indicated. The absorption coefficient at the center of a Lorentz line with $\alpha = 0.1$ cm^{-1} is represented by k_{max}. The curve which represents a sample at 431°K is based on a line whose strength is the same at 431°K as at 296°K with k_{max} equal to the absorption coefficient at the center of the line when the sample is at 296°K.

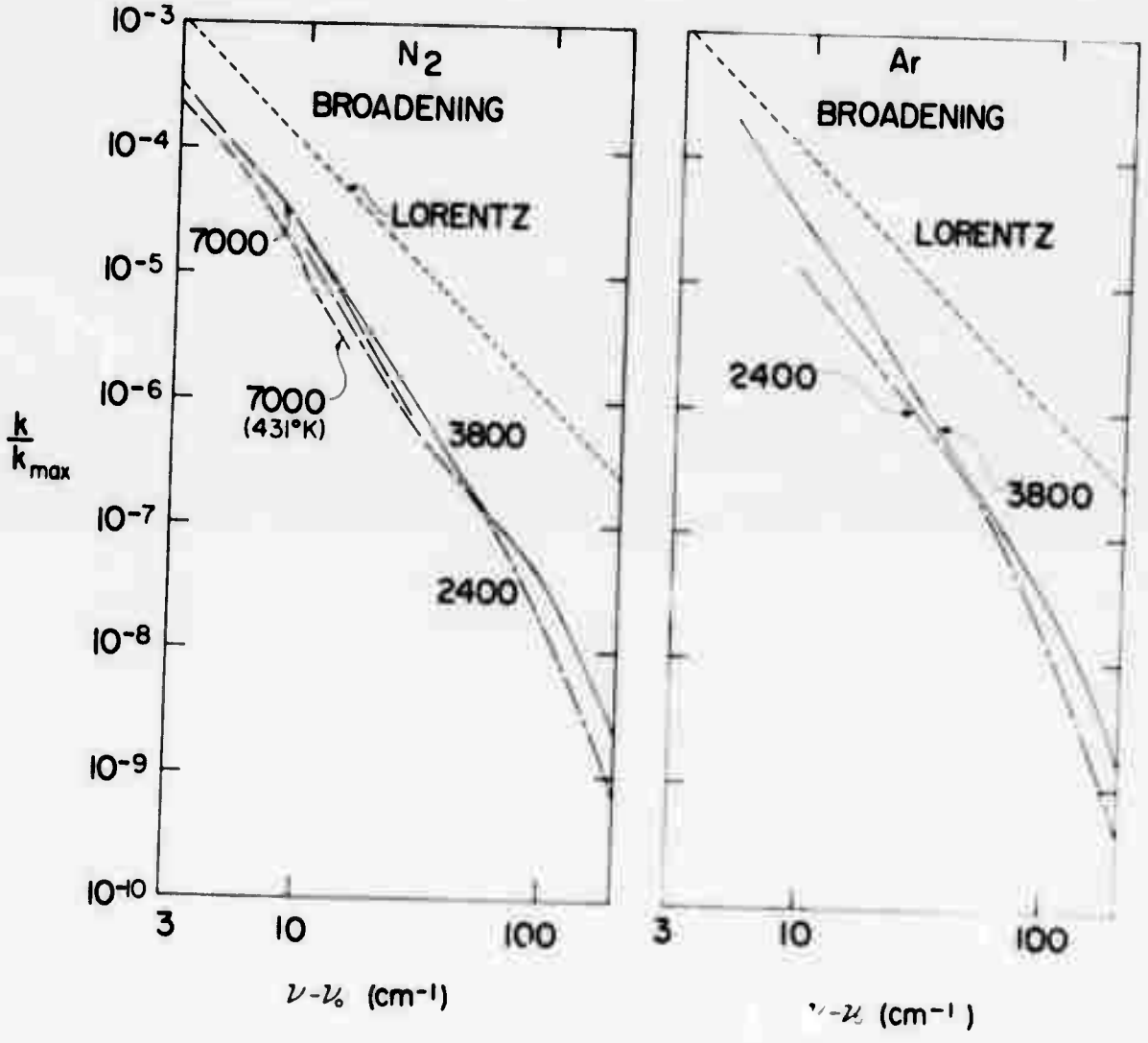

FIG. 18. Ratio k/k_{max} versus $(\nu-\nu_o)$ for N_2- and A-broadened lines in three spectral regions. The curves correspond to a Lorentz line and to lines in the wavenumber regions indicated. k_{max} is the absorption coefficient at the center of a Lorentz line with $\gamma = 0.1$ cm^{-1}.

Preceding page blank

the order of increasing wavenumber. This phenomenon may be based on the ratio of the period of the electromagnetic waves to the time the colliding molecules are within a certain distance.

INFLUENCE OF X ON CALCULATED LINE STRENGTH

It is apparent that if X is less than unity for all $(\nu-\nu_o)$, Eq. (4) cannot be satisfied exactly, and the line strength S given by Eq. (5) will depend on pressure and on the broadening gas. Experience has shown us that line strengths are not functions of pressure or broadening gas; therefore, we must consider the validity of the method used to derive the curves of X versus $(\nu-\nu_o)$ with respect to the condition of constant line strength. If pressures are low and α is many times less than the minimum value of $(\nu-\nu_o)$ for which $X = 1$, the integral of the right hand side of Eq. (8) is barely changed when the non-unity values of X are included. However, if α is larger, the influence of substituting X into Eq. (8) is not negligible.

This phenomenon is illustrated in Fig. 19, where Curve A represents a Lorentz line with $\alpha = 1\ cm^{-1}$, which corresponds to a typical self-broadened line at a pressure of approximately 10 atm. Curve B represents

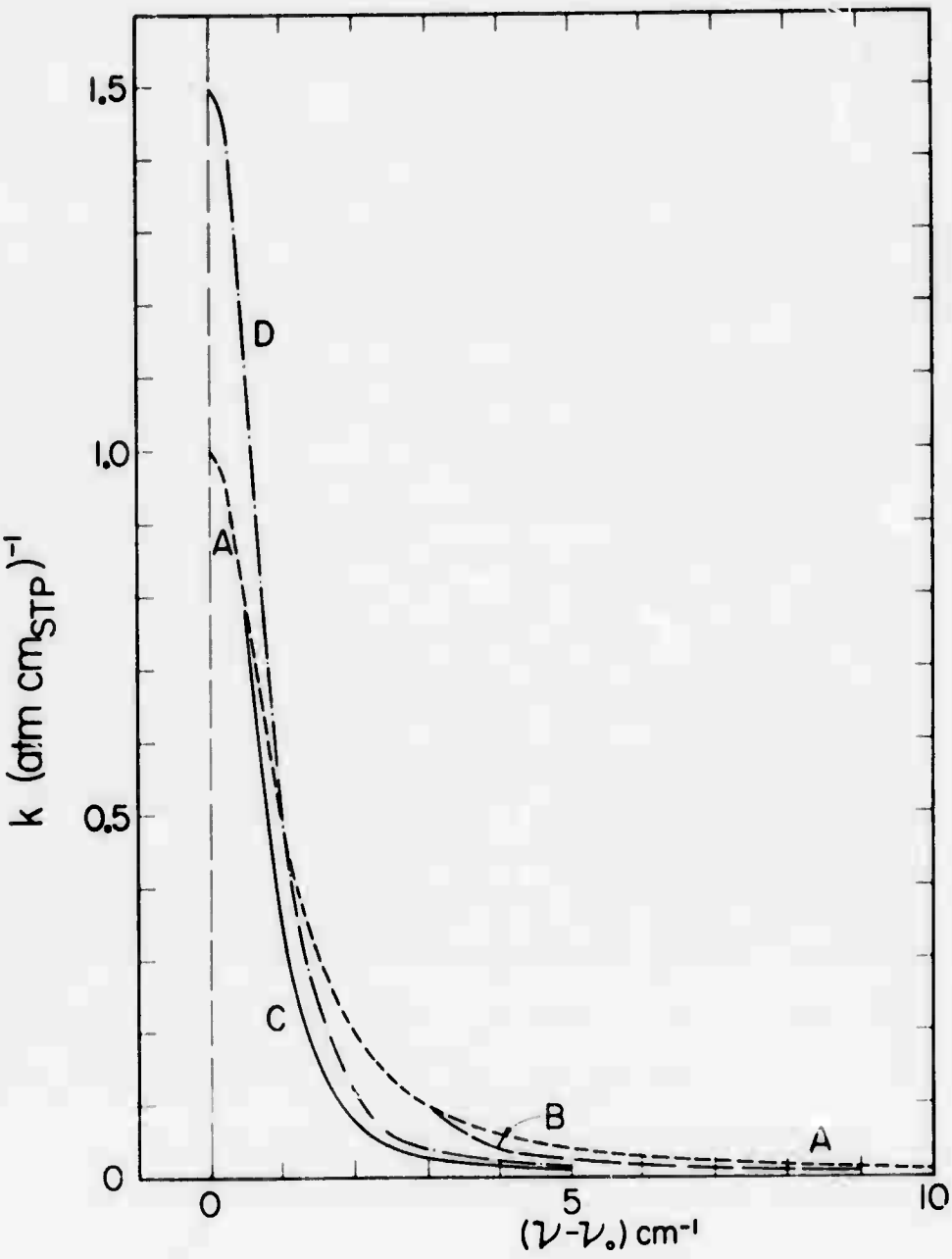

FIG. 19. k plotted versus $(\nu-\nu_o)$ to show influence of Y on $\int k d\nu$ for a single line. Curves A and B represent a Lorentz line and a CO_2 line in the 7000 cm^{-1} region, respectively, with γ = 1 cm^{-1} and k_{max} = 1(atm cm$_{STP}$)$^{-1}$. Curve C was obtained by multiplying A by values of Y given in Fig. 12 for N_2 lines. Curve D was obtained by multiplying C by the appropriate factor, 1.5, so that the area is the same under Curves A and D. The curves are shown for $(\nu-\nu_o) \leq 10$ cm^{-1} only, but larger $(\nu-\nu_o)$ were considered when calculating the areas under the curves.

the absorption coefficient of such a line after it has been modified according to the curve of χ versus $(\nu-\nu_o)$ for a self-broadened CO_2 line in the 7000 cm^{-1} region. Curve B is coincident with Curve A for $(\nu-\nu_o) < 3$ cm^{-1}. We see that the area under Curve B, which represents the $\int k d\nu$, is not greatly different from that under Curve A, so that the factor χ in Eq. (8) has only a moderate influence on the line strength. Approximately 0.065 of the total $\int k d\nu$ for a Lorentz line occurs for $|\nu-\nu_o| \geq 10\ \alpha$, the distance to which the curves in Fig. 19 have been drawn. Curve C represents an N_2-broadened line with $\alpha = 1$ cm^{-1} after it has been modified according to the curve of χ for N_2 broadening in the 7000 cm^{-1} region. The area under Curve C is only two-thirds the area under Curve A. Therefore, it is apparent that the profile over all values of $(\nu-\nu_o)$ cannot be given by Eq. (8) with χ a function of $(\nu-\nu_o)$ only if the strength of the line is independent of pressure.

Since Eq. (8) is not appropriate for all conditions, we will consider the applicability of a slightly more complex relationship to a wider range of α and $(\nu-\nu_o)$. We define

$$\Phi(\chi,\alpha) = \int k d\nu / \int k_L\, \chi(\nu-\nu_o) d\nu,$$

where k_L corresponds to a Lorentz line. For a given χ function and a given α, the absorption coefficient due to a single line is given by

$$k = k_L\, \Phi(\chi,\alpha)\, \chi(\nu-\nu_o). \tag{13}$$

The quantity $\varphi(X,\alpha)$ is adjusted so that $\int k(\nu)$ is independent of pressure or broadening gas. Since $X \leq 1$, φ must be ≥ 1 and increase with increasing α. In the example of the N_2-broadened line given in the preceding paragraph, φ is $1 \div 2/3 = 1.5$, and k is represented by Curve D, which was obtained by multiplying the values in Curve A by 1.5.

A test of the validity of Eq. (13) for a region including strong lines was made from measurements on several samples in the R-branch of the $10^0 1$ band from approximately 3720 to 3740 cm^{-1}. The integral of the observed absorption coefficient, $\int k d\nu$, over this region was found to be the same, within 2 or 3% experimental error, whether the lines were self-broadened, N_2-broadened, or He-broadened. Furthermore, this quantity was essentially the same for samples at 8 atm as at 15 atm, indicating that the sum of the strengths of all of the lines is independent of the broadening gas or the pressure, as assumed.

We assumed that Eq. (13) was valid and calculated k and $\int k d\nu$ over the 3720-3740 cm^{-1} region for sample parameters corresponding to the samples of pure CO_2, CO_2 + N_2 and CO_2 + He studied. Values of X from Fig. 13 were included in the calculations, and the appropriate values of $\varphi(X, \alpha)$ were determined for substitution into Eq. (13) by the procedure followed in obtaining Curve D of Fig. 19. The agreement between the calculated and observed values was good, indicating that Eq. (13) could be used in a region where the absorption is due to nearby, strong lines. The calculated values were also essentially the same as those calculated for the same samples on the assumption that the Lorentz shape was valid. This apparent

lack of dependence on line shape occurs because essentially all absorption in this region (3720-3740 cm^{-1}) is due to nearby lines and, therefore, independent of the shape of the extreme wings, provided $\int k d\nu$ within a few cm^{-1} of the center for each line remains constant.

If the relationship given by Eq. (13) is valid, the absorption coefficient in the extreme wings of lines must increase more than linearly with pressure. For example, α for a typical N_2-broadened line at 1 atm, is approximately 0.08 cm^{-1}, and the Lorentz line shape is valid for $(\nu-\nu_o)$ less than approximately 7 α. Therefore, the modification brought about by multiplying by χ for $(\nu-\nu_o) > 0.5$ cm^{-1} causes only a small change in $\int k d\nu$, and $\varphi \cong 1$. But, as we have shown immediately above, at approximately 12 atm the half-width is 1 cm^{-1} and $\varphi = 1.5$. Therefore, if Eq. (13) is valid, k in the extreme wings of the line is 1.5 x 12 = 18 times as great for 12 atm as for 1 atm. We have measured the absorption coefficient for both self and N_2 broadening for samples covering wide ranges of pressure and have found no such super-linear relationship between absorption coefficient and pressure. All of our results indicate that the absorption coefficient increases linearly with pressure when the absorption is due to lines whose centers occur at a distance of several half-widths. Therefore, we conclude that the absorption coefficient in the wings cannot be represented properly by Eq. (13).

Most of the discussion in this section has applied to situations in which α is not a small fraction of the minimum value of $(\nu-\nu_o)$ at which there is significant deviation from the Lorentz shape. Under these situations we find that Eq. (8) is not valid if we assume that χ is a function

of $(\nu-\nu_o)$ only. We have found further that the shape of the extreme wings cannot be represented by Eq. (13). More information than can be obtained by the methods used in the present study are required before the shapes of lines within approximately 5 cm^{-1} of their centers can be understood. However, it should be noted that Eq. (8) is applicable with χ a function of $(\nu-\nu_o)$ when this quantity is more than a few cm^{-1} and pressures are less than 1 or 2 atm. As the pressure increases this relationship is still appropriate if $(\nu-\nu_o)$ is several times as great as α.

SUGGESTED FURTHER WORK

The need for several additional experiments is apparent from the results and the conclusions which can be drawn about the shapes of CO_2 absorption lines. Similar experiments should be done for absorption bands of gases such as CO or N_2O which have sufficiently sharp band heads that wing absorption can be measured without excessive interference by nearby lines. Additional information could be obtained from similar measurements near Q-branches of several gases, including CO_2 near 670 cm^{-1}.

The stronger-than-expected dependence of wing absorption on temperature needs further investigation over wider temperature ranges, above and below room temperature. Additional knowledge about the influence of temperature is required in order to make reliable calculations of heat transfer in atmospheres which contain considerable CO_2, such as Mars and Venus. Measurements of the absorption near 875 cm^{-1} by the extreme wings of lines at lower wavenumbers for high-pressure samples might also provide

additional information about the previously unexpected dependence of wing absorption on wavenumber. On the basis of comparisons made in Figs. 17 and 18, we expect the wings of the distant lines contributing to the absorption near 875 cm^{-1} to deviate even further than the lines included in the present study from the Lorentz shape. The very weak absorption by the wings of lines broadened by H_2 and He is surprising and should be investigated further in other spectral regions and with other absorbing gases.

The present investigation has provided little more than qualitative information about the shapes of lines between 0.5 and 5 cm^{-1} from their centers. The region near the band head at 6988.56 cm^{-1} could provide additional information for this portion of the lines if measurements were made with spectral slitwidths less than approximately 0.05 cm^{-1}, which is considerably narrower than we could attain. Wavenumber accuracy of approximately 0.01 cm^{-1} would also be required. With these experimental conditions the half-widths of the lines very near the band head could be measured and their contribution to the absorption just above the band head could be determined much more accurately than has been done in the present study.

Spectral scans made with very good resolution over regions containing lines could also provide valuable information about the relative shapes of lines within a few tenths of a cm^{-1} from their centers when broadened by different gases. The method illustrated by Fig. 5 in which two samples with different broadening gases, but the same absorber thickness, are employed can provide a direct comparison of the shapes of lines broadened by different gases without accounting for the distortion of the spectral curve because of finite spectral slitwidth.

All of the results obtained in the present study for the extreme wings of lines relate to the high-wavenumber side of the line centers ($\nu > \nu_o$). Since band heads are formed on the high-wavenumber sides of CO_2 bands, regions where most of the absorption results from distant lines occur above the line centers. There are no places in the spectrum where most of the absorption is due to the extreme wings of lines at higher wavenumbers. However, by making careful measurements on the low wavenumber sides of some of the bands for samples at several atm pressure, one could probably account for the nearby lines with sufficient accuracy to estimate the contribution due to stronger, distant lines. The shapes of the low-wavenumber sides of the lines ($\nu < \nu_o$) could not be determined as accurately as the high-wavenumber sides have been; however, certain limits on the possible asymmetry of the lines could be established. Measurements of this type might be made more accurately with samples containing a single isotopic species in order to reduce the contribution of weak isotopic lines which occur where the absorption would be measured. Since the most common isotope, $C^{12}O_2^{16}$, is lighter than the other isotopes of significant abundance, the isotopic bands usually occur on the low-wavenumber side of the stronger $C^{12}O_2^{16}$ bands with the same transitions. Cooling the samples to reduce the contribution by difference bands and by high J value lines would probably make more accurate measurements possible.

REFERENCES

1. A. A. Michelson, Astrophys. J. 2, 251 (1895).
2. W. S. Benedict, R. Herman, G. E. Moore, and S. Silverman, Can. J. Phys. 34, 830 and 850 (1956).
3. W. S. Benedict, R. Herman, G. E. Moore, and S. Silverman, Astrophys. J. 135, No. 1, 277 (1962).
4. B. H. Winters, S. Silverman, and W. S. Benedict, J. Quant. Spectry Radiative Transfer 4, 527 (1964).
5. D. E. Burch, D. A. Gryvnak, and R. R. Patty, J. Opt. Soc. Am. 57, 885 (1967).
6. G. Herzberg, Molecular Spectra and Molecular Structure II. Infrared and Raman Spectra of Polyatomic Molecules (D. Van Nostrand Co., Inc., Princeton, New Jersey, Ninth Printing 1960).
7. L. D. Gray and J. E. Selvidge, J. Quant. Spectry Radiative Transfer 5, 291 (1965).
8. D. E. Burch, D. A. Gryvnak, and R. R. Patty, J. Opt. Soc. Am. 58, 335 (1968).

REFERENCES (Continued)

9. R. P. Madden, J. Chem. Phys. 35, 2083 (1961).

10. D. E. Burch, E. B. Singleton, and D. Williams, Appl. Opt. 1, 359 (1962).

11. R. R. Patty, E. R. Manring, and J. A. Gardner, J. Opt. Soc. Am. (In press).

12. P. W. Anderson, Phys. Rev. 76, 647 (1949).

DOCUMENT CONTROL DATA - R&D

(Security classification of title, body of abstract and indexing annotation must be entered when the overall report is classified)

1. ORIGINATING ACTIVITY (Corporate author) Advanced Development Operation Aeronutronic Division Philco-Ford Corporation	2a REPORT SECURITY CLASSIFICATION Unclassified 2b GROUP

3. REPORT TITLE

The Shapes of Collision-Broadened CO_2 Lines

4. DESCRIPTIVE NOTES (Type of report and inclusive dates)

Scientific Report

5. AUTHOR(S) (Last name, first name, initial)

Burch, Darrell E. Patty, Richard R.
Gryvnak, David A. Bartky, Charlotte E.

6. REPORT DATE	7a TOTAL NO OF PAGES	7b NO OF REFS
31 August 1968	67	12

8a. CONTRACT OR GRANT NO. NOnr 3560(00) b. PROJECT NO. c. d.	9a ORIGINATOR'S REPORT NUMBER(S) U-3203 9b OTHER REPORT NO(S) (Any other numbers that may be assigned this report)

10. AVAILABILITY/LIMITATION NOTICES

11. SUPPLEMENTARY NOTES	12. SPONSORING MILITARY ACTIVITY

13. ABSTRACT

The shapes of the extreme wings of self-broadened CO_2 lines have been investigated in three spectral regions near 7000, 3800, and 2400 cm^{-1}. Absorption measurements have been made on the high wavenumber sides of band heads where much of the absorption by samples at a few atm is due to the extreme wings of strong lines whose centers occur below the band heads. Considerable new information has been obtained about the shapes of self-broadened CO_2 lines as well as CO_2 lines broadened by N_2, O_2, A, He, and H_2. Beyond a few cm^{-1} from the line centers all the lines absorb considerably less than Lorentz-shaped lines having the same half-widths. The deviation from the Lorentz shape decreases with increasing wavenumber in going from one of the three spectral regions to the next. The absorption by the wings of H_2- and He-broadened lines is particularly low, and the absorption decreases with increasing temperature at a faster rate than predicted by existing theories.

DD FORM 1 JAN 64 1473

14 KEY WORDS	LINK A		LINK B		LINK C	
	ROLE	WT	ROLE	WT	ROLE	WT
CO_2 Line Shape Line Broadening						

INSTRUCTIONS

1. ORIGINATING ACTIVITY: Enter the name and address of the contractor, subcontractor, grantee, Department of Defense activity or other organization *(corporate author)* issuing the report.

2*a*. REPORT SECURITY CLASSIFICATION: Enter the overall security classification of the report. Indicate whether "Restricted Data" is included. Marking is to be in accordance with appropriate security regulations.

2*b*. GROUP: Automatic downgrading is specified in DoD Directive 5200.10 and Armed Forces Industrial Manual. Enter the group number. Also, when applicable, show that optional markings have been used for Group 3 and Group 4 as authorized.

3. REPORT TITLE: Enter the complete report title in all capital letters. Titles in all cases should be unclassified. If a meaningful title cannot be selected without classification, show title classification in all capitals in parenthesis immediately following the title.

4. DESCRIPTIVE NOTES: If appropriate, enter the type of report, e.g., interim, progress, summary, annual, or final. Give the inclusive dates when a specific reporting period is covered.

5. AUTHOR(S): Enter the name(s) of author(s) as shown on or in the report. Enter last name, first name, middle initial. If military, show rank and branch of service. The name of the principal author is an absolute minimum requirement.

6. REPORT DATE: Enter the date of the report as day, month, year; or month, year. If more than one date appears on the report, use date of publication.

7*a*. TOTAL NUMBER OF PAGES: The total page count should follow normal pagination procedures, i.e., enter the number of pages containing information.

7*b*. NUMBER OF REFERENCES: Enter the total number of references cited in the report.

8*a*. CONTRACT OR GRANT NUMBER: If appropriate, enter the applicable number of the contract or grant under which the report was written.

8*b*, 8*c*, & 8*d*. PROJECT NUMBER: Enter the appropriate military department identification, such as project number, subproject number, system numbers, task number, etc.

9*a*. ORIGINATOR'S REPORT NUMBER(S): Enter the official report number by which the document will be identified and controlled by the originating activity. This number must be unique to this report.

9*b*. OTHER REPORT NUMBER(S): If the report has been assigned any other report numbers *(either by the originator or by the sponsor)*, also enter this number(s).

10. AVAILABILITY/LIMITATION NOTICES: Enter any limitations on further dissemination of the report, other than those imposed by security classification, using standard statements such as:

(1) "Qualified requesters may obtain copies of this report from DDC."

(2) "Foreign announcement and dissemination of this report by DDC is not authorized."

(3) "U. S. Government agencies may obtain copies of this report directly from DDC. Other qualified DDC users shall request through

_____."

(4) "U. S. military agencies may obtain copies of this report directly from DDC. Other qualified users shall request through

_____."

(5) "All distribution of this report is controlled. Qualified DDC users shall request through

_____."

If the report has been furnished to the Office of Technical Services, Department of Commerce, for sale to the public, indicate this fact and enter the price, if known.

11. SUPPLEMENTARY NOTES: Use for additional explanatory notes.

12. SPONSORING MILITARY ACTIVITY: Enter the name of the departmental project office or laboratory sponsoring *(paying for)* the research and development. Include address.

13 ABSTRACT: Enter an abstract giving a brief and factual summary of the document indicative of the report, even though it may also appear elsewhere in the body of the technical report. If additional space is required, a continuation sheet shall be attached.

It is highly desirable that the abstract of classified reports be unclassified. Each paragraph of the abstract shall end with an indication of the military security classification of the information in the paragraph, represented as *(TS)*, *(S)*, *(C)*, or *(U)*

There is no limitation on the length of the abstract. However, the suggested length is from 150 to 225 words.

14. KEY WORDS: Key words are technically meaningful terms or short phrases that characterize a report and may be used as index entries for cataloging the report. Key words must be selected so that no security classification is required. Identifiers, such as equipment model designation, trade name, military project code name, geographic location, may be used as key words but will be followed by an indication of technical context. The assignment of links, rules, and weights is optional.

GPO 886-551

PHILCO-FORD CORPORATION
Aeronutronic Division
Newport Beach, Calif. • 92663